

Inner Shell Spectroscopy (ISS)

<u>Local team</u>	<u>Scientific and technical advisors</u>
<p>Bruce Ravel, Spokesperson bravel@bnl.gov, 631-344-3613 National Institute of Standards and Technology 100 Bureau Drive, Gaithersburg, MD 20899</p>	<p>Bruce Bunker, Professor (574) 631-6386, bunker@nd.edu 225 Nieuwland Science Hall Notre Dame University, Notre Dame, IN 46556</p>
<p>Anatoly Frenkel, Professor, (212) 340-7827, anatoly.frenkel@yu.edu Department of Physics, Yeshiva University 245 Lexington Avenue, New York, NY 10016</p>	<p>Mark Chance, Professor (216) 368-4406, mark.chance@case.edu Case Western Reserve University School of Medicine, Cleveland, Ohio 44106-4988</p>
<p>Jen Bohon, Biophysicist (631) 344-4613, jbohon@bnl.gov Case Western Reserve University NSLS, Building 725, BNL, Upton, NY 11973</p>	<p>Simon Bare, Senior Principal Scientist (847) 391-3171, simon.bare@uop.com UOP LLC, A Honeywell Company 25 East Algonquin Road, Des Plaines, IL 60017</p>
<p>Joseph Woicik, Physicist woicik@bnl.gov, 631-344-4247 National Institute of Standards and Technology 100 Bureau Drive, Gaithersburg, MD 20899</p>	<p>Chris Glover, Principal Scientist, XAS Beamline +61 3 85404142, chris.glover@synchrotron.org.au Australian Synchrotron 800 Blackburn Rd, Clayton VIC 3168, Australia</p>
<p>Lonny Berman, Physicist (631) 344-5333, berman@bnl.gov NSLS, Building 725, BNL Upton, NY 11973</p>	<p>Gerald T. Seidler, Professor (206) 616-8746 Physics Department University of Washington, Seattle, WA 98195</p>
<p>Paul Northrup, Research Scientist (631) 344-3565, northrup@bnl.gov Department of Geosciences Stony Brook University, Stony Brook, NY 11794</p>	<p>Serena DeBeer, Assistant Professor (607) 255-2352, sdg63@cornell.edu Chemistry and Chemical Biology Cornell University, Ithaca NY 14853</p>
<p>Trevor A. Tyson, Professor (973) 642-4681, tyson@adm.njit.edu Dept. of Physics, New Jersey Institute of Technology Newark, New Jersey 07102</p>	<p>Wendy Mao, Assistant Professor (650) 723-3718, wmao@stanford.edu Geological & Environmental Sciences Stanford University, Stanford, CA 94305</p>
	<p>Shelly Kelly, Physicist (123) 456-7890, dr.skelly@gmail.com EXAFS Analysis 719 Crestview Dr., Bolingbrook, IL 60440</p>
	<p>Satish Myneni, Associate Professor (609) 258-5848, smyneni@princeton.edu Department of Geosciences Princeton University, Princeton, NJ 08544</p>
	<p>Bhoopesh Mishra, Assistant Physicist (630) 252-7376, bhoopeshm@gmail.com Bioscience Division, Argonne National Laboratory Argonne, IL 60439</p>

Scientific justification for the ISS beamline

The unprecedented brightness and flux of NSLS-II will enable measurements with the high spatial, energy, and time resolution necessary to fully characterize ... complex systems. Advanced capabilities will include ... application of new experimental techniques, such as high-resolution x-ray emission spectroscopy and x-ray Raman scattering, to provide new spectroscopic information; and the use of combinatorial methods for large scale screening of novel materials.

NSLS-II CD-0 document

Absorption of an X-ray by an atom is one of the fundamental interactions of light with matter and the measurement of absorption is one of the core competencies of any synchrotron. X-ray absorption spectroscopy (XAS) has a long history at NSLS – many of the first beamlines on the NSLS X-ray ring were for XAS and the XAS community has remained large and productive for the entire 25 year history of NSLS. In that time, the use of XAS has become commonplace in a very wide variety of academic and industrial disciplines ranging from the life and environmental sciences to materials physics and chemistry, engineering materials, geophysics, and more. The XAS community at NSLS, however, operates within certain constraints.

The dilution of an absorber, the speed at which an XAS spectrum may be collected, and the effective use of high energy resolution spectrometers are the boundaries within which the NSLS XAS community currently operates. Each of these boundaries can be pushed back in significant ways by a high-flux source. This proposal is for a wiggler-based beamline dedicated to XAS and other inner shell spectroscopies. The exceptional flux provided by a wiggler enables measurement of absorber concentrations at environmentally or technologically relevant levels impractical to measure at dipole beamlines. Although a companion proposal (the TRS beamline) focuses on sub-second, time-resolved XAS, this beamline allows collection of high-quality XAS spectra in well under a minute and is an important part of the strategy for mitigating sample damage under the elevated flux. Finally, the high flux from the wiggler offers the use of point-to-point focusing and wavelength dispersive spectrometers, enabling collection of high-resolution XANES spectra, X-ray emission (XES) spectra, and the measurement of low-energy absorption edges via X-ray energy loss spectroscopy (XELS), all of which are shown schematically in Fig. 1.

Hard X-ray XES and XELS remain underused by the spectroscopy community not for lack of need or lack of interest but because of the complexity of the instrumentation and scarcity of beamlines at which such spectrometers are a routine part of the user program. In recent years, much progress^{1,2} has been made in both spectrometer design and integration into beamline experimental programs. The science examples shown below are a glimpse at the vast sweep of science that uses inner shell spectroscopy and which benefit by the

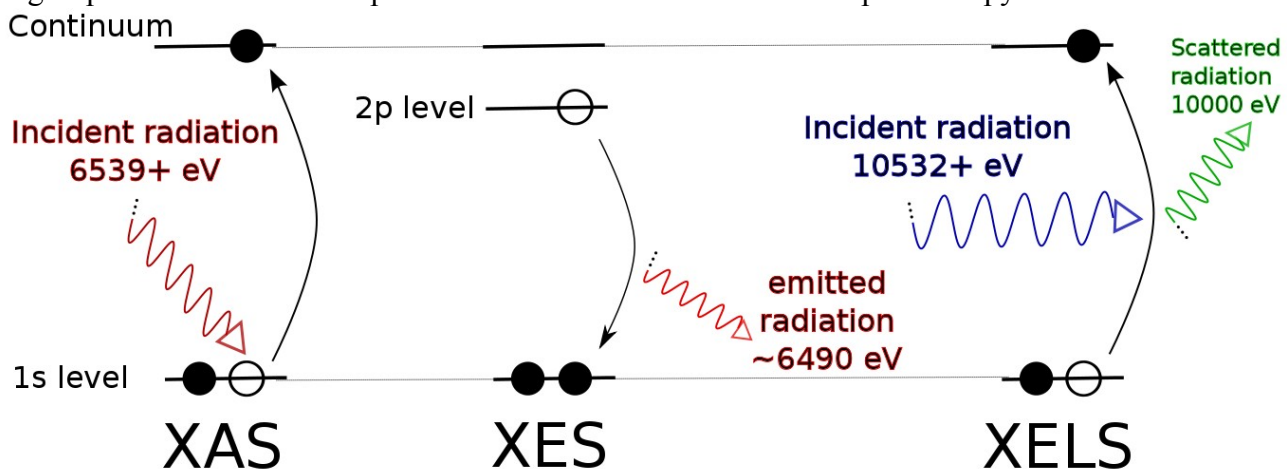


Figure 1: Schematic comparing the XAS, XES, and XELS measurements. In XAS, a deep core electronic excitation, the Mn K edge in this case, is measured by directly absorbing an incident photon. In XES, an electron fills the hole vacated in the XAS process and a photon is emitted. Shown here is the Mn K β emission from a 2p (or possibly some other high-lying) level following the Mn K edge XAS. In XELS, a photon is scattered inelastically with the energy lost used to promote a deep core electron. Shown here, an oxygen K edge (1s electron) is measured by XELS. The spectrometer in this example is tuned to 10 keV and the incident photon energy is scanned through the O K edge energy + the incident energy.

availability of the full complement of inner shell techniques. ISS combines the exceptional flux provided by an NSLS-II wiggler source, the highest quality conventional XAS, and the next generation of XES and XELS spectrometers into a world-class facility for X-ray spectroscopy as promised in the quote above taken from the founding document of the NSLS-II project.

Science case: XAS with very low absorber concentration

Biological science: Physiologically relevant concentrations of biomolecules are typically in the sub μM range, below the sensitivity of a standard XAS beamline. Thus these molecules are generally purified and concentrated for XAS measurement. Many biological samples cannot be forced into higher concentrations as they precipitate or form aggregates that are non-biologically relevant or inactive. In order to measure metalloprotein samples in biologically relevant concentrations, high flux is required, along with highly sensitive fluorescence detection. Rapid collection of data required for high-quality EXAFS of low concentration absorbers is of immense benefit to the life science community.

The use of high flux requires damage mitigation strategies. One such strategy uses continuous-flow regeneration of fresh sample in solution state, requiring significant volumes of sample but accommodating standard fluorescence detection. This strategy also allows for rapid mixing and stopped- or continuous-flow time-resolved experiments which can reach as low as the sub-millisecond time regime when full mixing of reactants can be achieved on this time scale.³ Cooling of the fluid to near freezing can aid in the reduction of reaction rates, increasing the number of relevant measurable reactions. The mixing time depends on the speed at which the sample is flowed and the distance of the incident beam from the mixing point, as depicted in the inset to Fig. 2 while the time resolution is defined by the size of the beam.

A significant number of enzymatic reactions critical for biological function occur on the ms to second time scales, particularly when cooled to near freezing temperatures. In general, these are reactions requiring conformational changes in a protein rather than those which need only perform electron transfer. Freeze-quench experiments⁴ have been used to probe the metal active site chemistry (Fig. 2) of those biomolecules which could be successfully concentrated without perturbation of function. The ISS beamline allows similar measurements under physiologically relevant concentrations, significantly increasing the number of systems amenable to investigation.

Environmental science: In a recent XAS experiment at APS (10ID), the adsorption of Hg to *Bacillus subtilis* and *Shewanella oneidensis* MR-1 biomass was investigated to understand the interaction of Hg with bacterial cell surfaces. A wide range of Hg^{2+} concentration (120 nM to 350 μM) was measured at a fixed bacterial cell density (2g/L of wet mass) and pH (5.5 ± 0.2). The measurements were performed using a tapered undulator delivering $\sim 2 \cdot 10^{12}$ ph/sec to the sample.

The Hg L(III) edge XAS analysis showed that Hg complexes entirely with sulfhydryl groups at the nanomolar and low micromolar concentrations, and with carboxyl sites at high micromolar concentrations (Fig. 3). Since Hg-cysteine complexes in aqueous solutions are known to exert strong influence on Hg-methylation⁵, cell surface bound Hg-(cysteine)₃ complexes at environmentally relevant Hg-biomass ratios are likely the key bottleneck in controlling the rate and extent of Hg-methylation. These results provide first ever insight on the mechanisms of the transfer of Hg to the cell cytoplasm through the cell membrane for intracellular processes like methylation⁶. At Hg concentrations above 15 μM , which required hours of measurements at an undulator

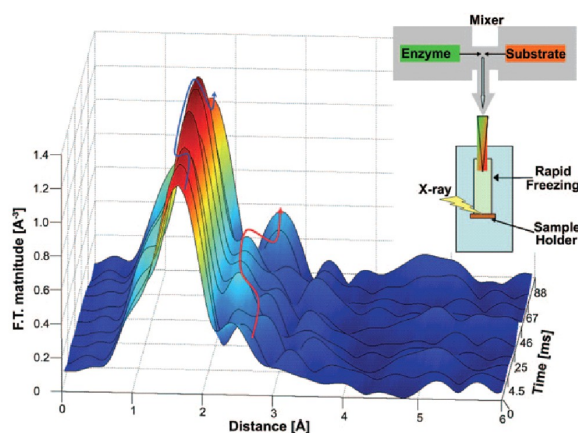


Figure 2: Figure XI. Time-resolved XAS measurements of TACE (a Zn-binding signal transduction control enzyme) during enzymatic catalysis using freeze-quench technology.⁴ Changes in Zn coordination and charge state were observable to 88 ms. The inset shows a schematic of a micro-fluidic mixer.

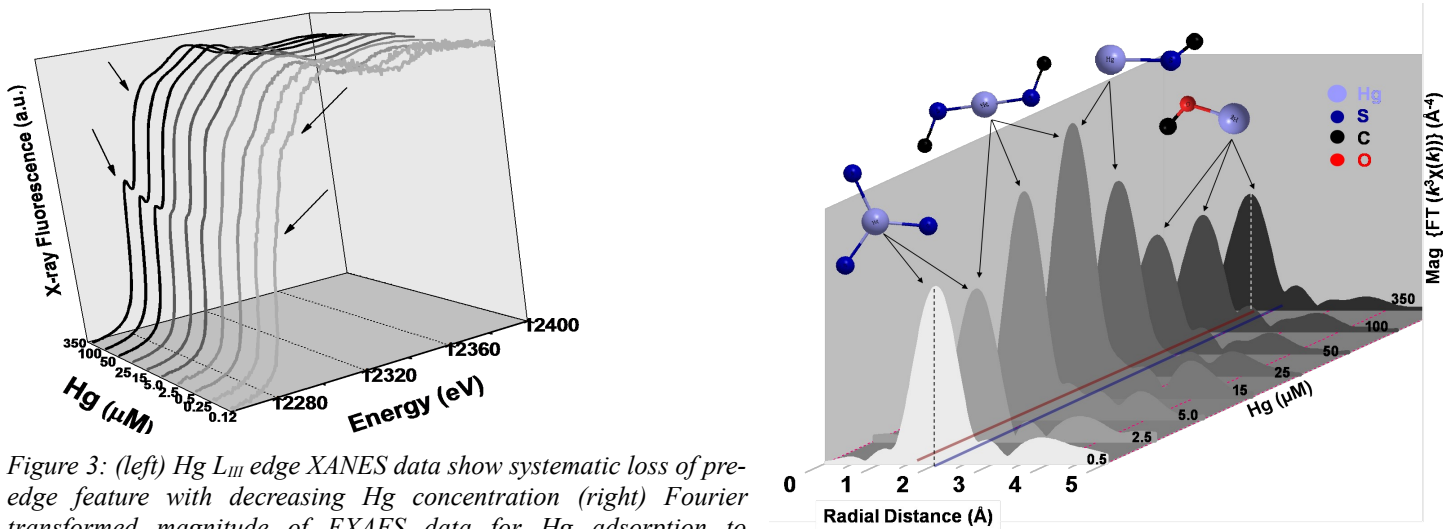


Figure 3: (left) Hg L_{III} edge XANES data show systematic loss of pre-edge feature with decreasing Hg concentration (right) Fourier transformed magnitude of EXAFS data for Hg adsorption to *Shewanella oneidensis* MR-1 as a function of adsorbed Hg concentration at pH 5.5 (± 0.2). The red and blue lines in the Fourier transform magnitude of EXAFS data correspond to 2.02 and 2.51 Å (phase corrected), respectively. A systematic change in the binding of Hg from Hg-S₃, Hg-S to Hg-carboxyl complex was observed with increasing Hg concentration in EXAFS spectra, a trend that was observed for all bacterial species examined. Cell density in this study was 10^{10} cell/L.

beamline with the flux of $\sim 2 \cdot 10^{12}$ and would have been impossible at dipole beamlines, low abundance sulfhydryl sites are saturated and masked by high abundance low affinity carboxyl sites which are not relevant to the intracellular biochemical processes. With the superior flux of ISS, measurement of environmentally relevant, low concentration samples will be routine for environmental contaminants across the periodic table.

Materials science: Thin films are not getting thicker, and dopants are not getting more concentrated. In the multi-billion dollar semiconductor industry, the “Grand Challenge” is to develop an alternative to the SiO₂ gate dielectric that has enabled Moore's Law scaling of the density of transistors in integrated circuit devices for the past 40 years. Higher speed with lower power consumption is no longer attainable with ultrathin (<2nm) SiO₂ gate dielectrics due to their high direct tunneling leakage currents. Future solutions require advances in new materials and nano-engineering, for example transistors for logic devices formed from conventional planar complimentary metal-oxide-semiconductor (CMOS)⁷ as well as novel architectures such as FinFETs to address scaling limits of planar CMOS. These devices are composed of ultra thin layers, with thicknesses approaching interfacial dimensions of ~ 1 nm.

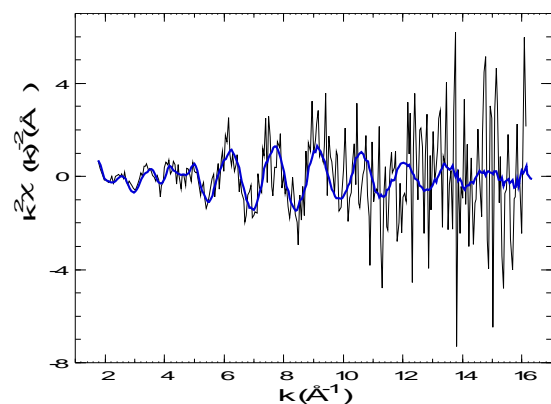


Figure 4: Ga K edge EXAFS from a 53 Å Ga_{0.26}In_{0.74}As alloy grown on an InP(001) substrate recorded at glancing-incidence. A single scan of ~ 20 minutes (black) is compared to the merged EXAFS (blue) from the same sample after 4 days of data collection on NSLS X23A2.

Bringing new semiconductor products to market requires quantitative local structural analysis on the atomic scale in device layers that are typically buried, thus inaccessible to many common microscopies. At an NSLS XAS beamline, high quality data on nanometer films can be collected over the course of several days, as shown in Fig. 4. The difficulty arises from the background due to the substrate and capping layers that support the film and to the low count rates attained due to the limited amount of material, that is, thinness of the films and diluteness of the dopants. For good signal to background, the films are studied at glancing incidence requiring beams as small as ~ 0.1 mm in at least one dimension. The high flux of ISS along with advanced energy dispersive detection¹⁶ yields superior quality data to the 4-day measurement in Fig. 4 with about 1 hour of data collection. With ISS, the study of industrially relevant materials is routine.

Science case: XES and high resolution XANES

XAS is commonly used for the speciation of valence and chemical state. This analysis is based on the chemical-dependent edge shift as well as subtle differences in the features within a few eV of the edge. The energy resolution of the XAS experiment is determined both by the bandpass of the monochromator and by the intrinsic Lorentzian width of the element-specific, finite, core-hole lifetime. There is a crossover that occurs in the transition metals where the lifetime broadening of the core-hole exceeds the monochromator width⁸. Often the ability to distinguish subtle features of an XAS experiment is limited by the natural width of the absorbing element rather than by the resolution of the monochromator. This effect can be reduced by better defining the observed final-state energy of the electron-core hole pair decay channel.^{9,10,11} A spectrometer like the instrument in Ref. 11 is used along with the high flux of the ISS beamline for high-resolution XANES measurements, significantly improving the sensitivity to slight differences in chemical composition and local structure around absorbing atoms.

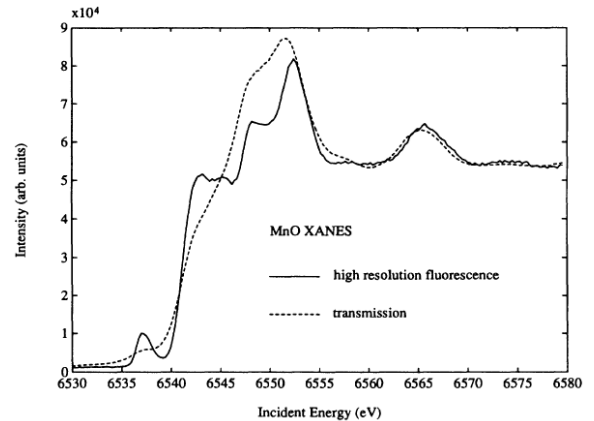


Figure 5: A conventional Mn K edge XAFS spectrum of MnO compared to a high-resolution spectrum from a high-resolution photon spectrometer.⁹

The same spectrometer is used to energy analyze the emission spectrum, revealing information about the electronic state of the absorber species that is complementary to what is obtained with XAS. Fig. 6 shows the very rich resonant emission spectrum through the absorber edge in CaF_3 . With the high flux of ISS and the miniXS spectrometer described in Appendix C, high quality 2-D RXES maps like the one shown can be achieved in ~ 5 minutes at ISS with individual exposures of 1-2 sec.

XES in industrial catalysis: In industrial research, throughput and efficiency is essential. Heterogeneous catalysts are regularly probed with a fluorescence microprobe, with μXAS measured at points of interest. With ISS, non-resonant X-ray emission spectroscopy (XES) measurement using the miniXS instrument (described in Appendix C) are feasible over an *entire* 2D region.

The performance of a Co catalyst used to produce ultra-low sulfur gasoline is positively correlated to the cobalt sulfidation. Mapping the location of the sulfided and oxidic Co within an extrudate is relevant to the development of these catalysts for industrial use. In Fig. 7, the XES spectra show a shift in the $\text{K}\beta_{1,3}$ peak depending on the ionicity/covalency of the Co bond. A sulfide bond has its $\text{K}\beta_{1,3}$ maximum at 2 eV lower in emission energy than an oxidized bond. At APS 20ID and with the current generation of miniXS detector, it took 30 seconds to acquire each XES spectrum in Fig. 7. A single image from the areal detector is shown in the inset. The x-ray emission intensities at each pixel are binned in energy to give the $\text{K}\beta$ emission spectrum. MiniXS uses a focused beam of ~ 50 μm to resolve the XES spectrum, which is a relevant length scale in these catalysts. With the high flux of ISS, the XES spectra shown in Fig. 7 take under a second. Thus the spatial distribution of sulfided/oxidized Co within a large, heterogeneous, thin section of catalyst material can be measured in hours, making measurement of real systems under real conditions quite feasible.

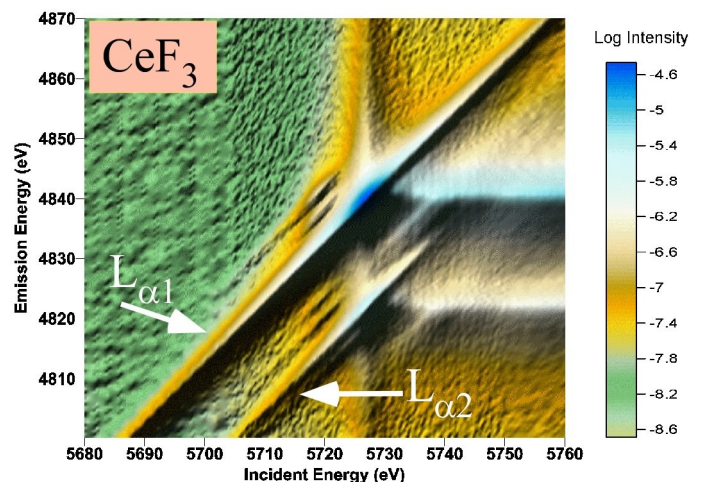


Figure 6: A 2-D RXES study for the Ce La emission of CeF_3 using the miniXS spectrometer at APS 20-ID. Note the strong splitting of the pre-edge resonance at ~ 5719 eV incident photon energy. The spectral characteristics in this energy range are useful indicators of the nature of the f-orbital ground states in such systems. Data courtesy R. Gordon (Univ. Washington).

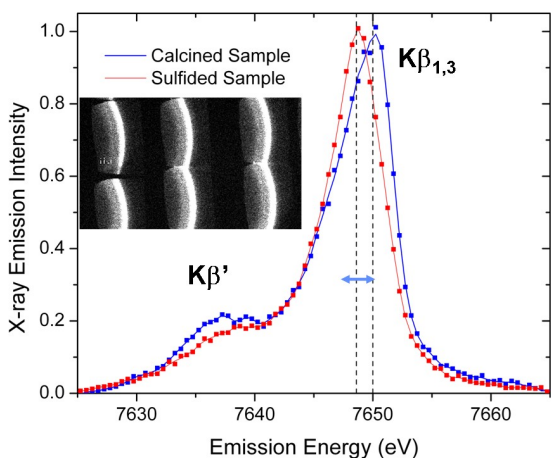


Figure 7: Non-resonant XES showing the shift in the $K\beta_{1,3}$ maximum x-ray emission energy depending on the sulfided or oxidized Co bonding environment. The inset shows the XES spectrum collected from in a single snapshot from the miniXS for one of the samples. The reflection from six crystals is shown.

which reacts with dioxygen to generate first a μ -peroxo-Fe(III)Fe(III) species (MMO-P), then a putative Fe(IV)Fe(IV) species (MMO-Q), which is responsible for oxidizing methane. Despite intense experimental and theoretical studies, MMO-Q and MMO-P have eluded structural characterization, and many questions about the nature of these intermediates remain. The experimental data for MMO-P have been used to argue for a cis- μ -1,2-peroxo bridging mode, while computational studies favor a μ - η^2 : η^2 -O₂ core. For MMO-Q the 2.5 Å Fe-Fe distance from EXAFS favors a bis- μ -oxo Fe(IV)-Fe(IV) diamond core structure. However, no vibrational data exist to support any of the postulated core structures and the mechanism for conversion of MMO-P to MMO-Q is unknown. There are many inherent challenges in studying these enzyme systems – relatively low concentrations (<1mM), incomplete conversion to the desired intermediates (~50-90%), and short reaction time scales. Many key insights into the reaction cycle of MMO can be obtained by using a combination K β XES on freeze-quench samples, site-selective XANES, and time-resolved XES on solutions using continuous/stop-flow methods. These are experiments that require the high flux of the ISS beamline. K β XES measurements are a probe of the Fe spin state. The K β valence to core (K $\beta_{2,5}$) region provides a selective probe of the Fe₂O₂ upper valence region and thus a sensitive measure of the oxygen bond strength and the binding mode. This is a unique means of characterizing these intermediates, which have eluded characterization by more conventional methods. By using the shifts in the K $\beta_{1,3}$ main line, one obtains site selective XANES and EXAFS to determine the electronic and geometric structure of the iron sites in differing oxidation states. This requires only moderate resolution (as the splitting between the K $\beta_{1,3}$ and K β' is ~15 eV), but requires high flux to access relatively low concentrations.

Ultimately, systems like MMO are ideal for time-resolved, dispersive XES studies using the miniXS instrument. This allows for the enzymatic transformation to be monitored in time (in the millisecond regime), as a function of spin state at the iron (from the K β main line), and changes in the valence to core region (which should provide insights into changes in the ligand/substrate binding). MMO has been studied by optical stop-flow methods, but the changes in optical spectra are difficult to relate directly to iron spin state and ligand environment, and are thus not readily correlated to structural changes or translated to mechanistic predictions.

Though MMO is used here to provide just one representative example, there are numerous cases where the ability to carry out K β XES, site-selective XANES and dispersive XES using miniXS (as in Fig. 6) in a time resolved fashion will provide key insights into biological reactions.

XES in Biochemistry: Heme and non-heme enzymes carry out a diverse array of metabolic transformations requiring the binding and activation of dioxygen. These include proteins such as methane monooxygenase (MMO) and others capable of C-H hydroxylations. These enzymes have generated intense interest aimed at understanding the mechanisms and nature of the active oxidizing species and the potential for translation to synthetic catalysts. In both model and enzyme systems, high-valent iron species are invoked as reactive intermediates. However, due the inherent reactivity of the synthetic and biological intermediates, the direct structural characterization is often elusive and spectroscopic identification has presented significant challenges. Inner shell spectroscopies are uniquely suited to address many questions of oxidation state, local geometry, and spin state of the active intermediates.

The active site of MMO is an example. The hydroxylation of methane is carried out by MMO found in methanotrophic bacteria. The soluble form of MMO uses a diiron active site

Science case: XELS – Soft X-ray edges measured with hard X-rays

X-ray energy loss spectroscopy (XELS) offers an enticing alternative to conventional soft X-ray spectroscopy. As shown in Fig. 1, the XELS measurement uses high energy incident X-rays and a spectrometer tuned to some high energy value. The incident beam is scanned through an energy range above the spectrometer tuning energy such that the difference between the incident and tuned energies passes through an absorption edge. In this way, the K edges of light elements, L and M edges of transition metals, and more exotic edges such as actinide N and O are measured. As the incident beam is highly penetrating, XELS is compatible with *in situ*, *operando*, and other sample environments as well as with wet samples and samples exposed to atmosphere. Furthermore, the XELS measurement is both bulk sensitive and unaffected by the self-absorption attenuation that can be problematic for soft x-ray spectra measured in fluorescence yield. As a result, XELS is an attractive complement to any soft x-ray spectroscopy measurement in any of the many scientific disciplines which use such measurements.

As an example, battery materials have long been the subject of study by XAS, including many lithiated compounds such as LiFePO_4 and $\text{Li}(\text{Ni},\text{Co})\text{O}_2$. To date, most spectroscopic studies have concentrated on the measurements of the transition metal K edge, including its measure in an *operando* environment, or *ex situ* measurements of the low-Z K edges or transition metal L edges. An XELS measurement offers the possibility of a more complete spectroscopic study of materials. Recent work at Argonne¹² has applied XELS to O K and transition metal L and M edge spectra in lithiated transition metals. All these *ex situ* experiments are readily transferred to the *operando* environment. XELS measurements of the various low energy edges in the battery system combined with the superb XAS capabilities of ISS provide a more complete spectroscopic picture of the behavior of the system. Oxides, nitrides, and carbides of transition and heavier metals are of interest to every spectroscopy-using discipline.

Beamline Concept

The ISS beamline is a wiggler-based beamline for Inner Shell Spectroscopies: XAS, XES, and XELS. This beamline delivers flux approaching 10^{14} photons/second, superior to any existing spectroscopy beamline and enabling science that is time-prohibitive or simply impossible on dipole sources.

This beamline uses the on-axis portion of a wiggler source with the following optical elements:

- vertical collimating mirror (VCM),
- double crystal monochromator (DCM)
- energy refining monochromator (ERM)
- toroidal focusing mirror (TFM).

The DCM operates in the range from 5 keV to 40 keV, delivers energy resolution of $\Delta E/E \approx 10^{-4}$ (typical for a Si(111) monochromator), and offers scan-to-scan variation in energy calibration under 0.05 eV. The ERM is a channel-cut Si(311) monochromator which can be placed in the beam to refine the energy resolution coming from the DCM for experiments which need it. The position of the beam delivered to the experimental hutch is stable to about 5 μm for proper operation of optics and spectrometers. In this sense, ISS benefits from the stability of the NSLS-II ring as well as from top-off operations. The TFM delivers a spot size of about 1 mm \times 0.3 mm at 9 keV.

The VCM and DCM are high heat load elements, requiring careful consideration of cooling strategies. Along with special design considerations (discussed in detail in Appendix A) for these components, use of ISS requires a variety of operational configurations (mirror angle and filter settings) designed to distribute heatload appropriately among the various elements when operating in different energy ranges. The configuration modes outlined in Appendix B serve as the model for operations at ISS.

The experimental hutch is a large end station with three experimental installations:

1. An upstream optical table for conventional XAS and the XES spectrometers, as described in Appendix CC, with energy discriminating detectors and ample room for additional equipment. A set of KB mirrors focuses to a $<50\ \mu\text{m}$ at 9 keV, preserving about 20% of full flux.
2. The XELS end station, modeled on the LERIX-2 instrument being developed by G.T. Seidler for the APS upgrade. This is described in full detail in Appendix D.
3. A large empty space at the downstream end for future instrumentation.

Choice of source

The ISS beamline requires a wiggler source. To explain this requirement, it is useful to divide the scientific mission of the ISS beamlines into two categories: (1) extensions of conventional XAS, particularly XAS measured with very low absorber concentration and (2) other spectroscopies, including high resolution XANES, XES, and XELS. The needs of these experiments are properly served by a wiggler and certain aspects of the ISS mission cannot be served by an NSLS-II undulator.

Extensions of conventional XAS: High flux enables difficult but otherwise conventional XAS experiments, for instance measurement of a sample with very low absorber concentration. An energy scanning experiment with an NSLS-II undulator requires synchronization with the monochromator (as is under investigation for the SRX beamline). For a high performance XAS beamline, the undulator solution is untenable. The small energy steps required in the XANES region would certainly strain the mechanical limitations of NSLS-II undulators.¹³ Synchronization likely limits the scanning rate far short of the requirements described below in the section on mitigating radiation damage. The trick of tapering the undulator, as at the APS, is impractical due to extreme loss of flux and the limited spectral band width from the tapered device. Furthermore, the high coherent flux of any undulator can amplify the effect of sample inhomogeneity on measurement linearity, damaging data quality at high photoelectron wavenumber¹⁴. **For superior conventional XAS performance, a wiggler is the only realistic option.**

Other spectroscopies: All point-to-point focusing and wavelength dispersive spectrometers work by explicitly coupling a spatial metric to energy resolution. As enhanced energy resolution comes at the necessary cost of instrumental throughput, high flux is required. The goal, then, is to maximize flux into a spot that delivers the energy resolution required for the experiment.

The peaks of the manganese $K\beta_{1,3}$ and $K\beta'$ emission lines shown in Fig. 8 are separated by $>15\ \text{eV}$ and each peak is $>5\ \text{eV}$ FWHM. A spectrometer resolution of $\sim 0.5\ \text{eV}$ is sufficient to measure these emission lines well. The XES spectrometers can provide that with a spot on the sample of $\sim 50\ \mu\text{m}$. The XELS spectrometer has a less stringent requirement of about $500\ \mu\text{m}$. A wiggler is bright enough for this application and delivers superior flux into the appropriately sized spot. **For a scientific program which combines XES and XELS with XAS of the highest quality, a wiggler is certainly the correct choice.**

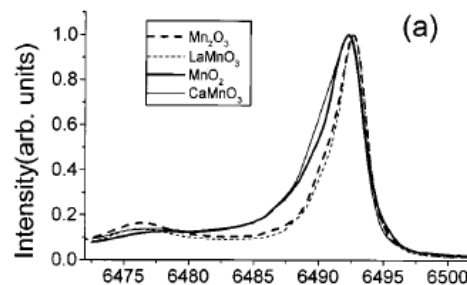


Figure 8: The Mn $K\beta$ emission from several Mn-containing materials. Tyson et al, *Phys Rev B* **60**:7 (1999) 4665.

Choice of wiggler

There are two options: (1) use an existing damping wiggler (DW) source, or (2) design a new wiggler type tailored to the needs of spectroscopy. Each option has merit.

The DW offers world-leading flux approaching 10^{14} photons/sec and already exists within the scope of the construction project. However the high heat load of the DW source requires the development of optics, masks and filters capable of sustaining these very high power loads.

In Appendix B we present the solution to the problem of handling the heat load from canted 3.5 m DW sources that was presented in 2008 as part of the proposed XAS Project Beamline. Although somewhat out of date with

respect to the current design of the NSLS-II DW, the concept in that Appendix offers an actionable approach for ISS. The earlier proposal would have delivered flux of over 10^{13} ph/sec, competitive with any spectroscopy beamline in the world. (See Fig. 12 on page 18.) This is the baseline, the lower bound of performance we expect for ISS. Appendix A outlines an approach requiring R&D to delivering truly world-leading flux from the DW source.

Alternately, a variable gap source could tune the critical energy and power distribution, thus minimizing some of the challenges associated with the DW source. Of course, any wiggler capable of producing the high flux required for a world-class spectroscopy beamline will require design of optical elements capable of supporting very high heat loads.

Regardless of choice of wiggler, this proposal benefits from work already undertaken by the NSLS-II project. The XPD beamline is developing windows and filters capable of absorbing significant heat load. ISS will use these developments. Calculations commissioned by NSLS-II from Accel show that a directly cooled glidcop mirror can support up to 7 kW incident heat, deforming with a slope error which remains approximately linear over the entire active surface of the mirror. (See Fig. 9 in Appendix A.) Although significant, this can be corrected dynamically, particularly given that top-off operations will assure that the heat load remains constant over time for a given mirror setting.

The wiggler XAS beamline at the Australian Synchrotron easily supports a 700 W load on a directly-cooled, Si(111) crystal. At SSRL, power as high as 1.1 kW with minimal thermal distortion to the first crystal have been demonstrated.¹⁵ As discussed further in Appendix A, this is a somewhat conservative approach to a high heat-load monochromator. Recent calculation show that a directly-cooled first crystal can support significantly higher heat-loads with manageable thermal distortion to the crystal. Additional R&D is required to understand the full impact of this thermal distortion on beam performance in terms of impact on flux, resolution, and positional spread.

Ultimately, it is the responsibility of the NSLS-II project to determine the optimal wiggler design for the ISS beamline. We on the proposal team recommend that the use of an existing DW source be considered as the first option. Strategies for mitigating many aspects of the heat load already exist. Other aspects, most notably the design of the DCM first crystal, are areas that will require R&D. At the least, a beamline that is competitive with the best spectroscopy beamlines in the world is clearly tenable. The prospect of delivering truly world-leading flux to the experimental station merits the technical risk associated with an R&D effort.

Detectors

Energy discriminating detection: Recent work¹⁶ demonstrates that the silicon drift detector (SDD) handles count rates up to $4 \cdot 10^5$ ph/sec/element with an energy resolution of around 220 eV at 6500 eV using analog signal chains with 0.1 μ sec shaping time. A multi-element SDD is the workhorse fluorescence detector for XAS.

For high energy edges such as 4d metal K edges, the SDD is inefficient due to the limited stopping power of the Si detection element. A large-area germanium detector (like the Canberra instruments at the CLS HXMA or Australian XAS beamlines) or the germanium drift detector being developed by the BNL Instrumentation Division is required.

Wavelength dispersive detection: The miniXS instrument, shown in Fig. 17 on page 22, uses an array of crystals scattering dispersively onto an area detector to measure a bandpass wide enough to cover entire fluorescence lines. This short working distance XES spectrometer requires an assortment of crystal carriages to cover different fluorescence energy ranges, as described in Appendix C. This spectrometer also requires a low background noise area detector. The large area [Pilatus 300K by Dectris](#) combines with the high flux of ISS to provide world-leading throughput for this non-resonant XES system.

The long working distance spectrometer is a proven technology, having been implemented at NSLS, SSRL, ESRF, CHESS, and elsewhere. It consists of an array of scattering elements on Rowland circles and focused onto a point or areal detector. A model for this instrument is the one in use at ESRF ID26,¹⁷ although with up to

10^{14} ph/sec on the sample, ISS outperforms ID26 by an order of magnitude. About 20% of this flux is preserved through the focusing optics for use by the spectrometers. A large array of spherically bent crystal analyzers are used for XELS measurements, as described in detail in Appendix D. An energy resolution of about 0.5 eV in the range of transition metal K β fluorescence is the target for this instrument, requiring the use of the ERM. Without the ERM, the energy resolution will be closer to 1.1 eV. This is a somewhat larger target than for similar instruments being proposed for NSLS-II or built elsewhere, but it is a wise target. 0.5 eV is sufficient resolution for both XES and XELS and that relatively large bandpass is appropriate for a high throughput instrument.

Mitigating radiation damage to the sample

With significant power (~100 mW) deposited onto the sample, radiation damage occurs quickly for many samples, especially especially organic or water-containing samples. Strategies for mitigating this problem are implemented deeply into the beamline concept. Low temperature sample containment is used for many experiments and all sample stages and spectrometers are designed to accommodate cryostats. More significantly, measurement strategies that minimize the exposure of the sample to the beam are adopted. The step scan conventionally used at XAS beamlines is problematic in that time spent stepping and settling motors is time spent exposing the sample to the beam without actually collecting data. At ISS, the standard mode of operation for XAS experiments, then, is the slew scan in which the mono is driven continuously in increasing energy and data is streamed into time-delimited bins. The shutter is closed as the mono rewinds and is opened for the subsequent scan. Given sufficiently large samples, the sample is periodically rastered to a new location, avoiding excessive exposure at any one spot. Individual EXAFS scans are typically be measured in about 20 seconds while XANES scans can be as short as 5 seconds.

Required Technical Advances

1. Optimization of optics and beamline configurations. Management of the high heat load from the wiggler source is the area most in need of R&D attention, particularly for the DW source. The range of configuration options and their consequence on each optical element must be explored to optimize performance over the entire operational range of the beamline.
 - a) Development of a high heat load VCM – likely to be made of Glidcop, directly cooled, and coated with Pt and Rh – capable of supporting as much as 7 kW incident heat load. This mirror will need to dynamically compensate for heat-induced figure error, which is calculated¹⁸ to be linear over the active surface of the mirror.
 - b) Development of a high heat load DCM. At the SSRL, a directly cooled Si(111) crystal was found¹⁵ to deform negligibly with heat loads as high as 1.1 kW. This should be the minimum target of the DCM R&D effort. As outlined in Appendix A, a directly cooled DCM can support very high heat load, although the effect of the thermal distortion on flux and other performance attributes must be explored. One particularly important area is stability of LN₂ flow which is known to be a serious source of systematic noise for cryo-cooled monochromators.
 - c) Development of an ERM. A secondary Si(311) mono to refine the energy resolution requires development of feedback and tracking system for effective, high-throughput operation.
 - d) Other high heat load components. ISS benefits by work done for the XPD Project Beamline.
 - e) Beamline configuration management software. Any array of beamline configurations as extensive as those listed in Appendix B will create substantial complexity of beamline operation. Optical configuration software, combining database look-up with optimization algorithms, will be required to make effective use of ISS with high user throughput.
2. Spectrometers compatible with many sample environments must be designed to meet the goal of applying the full suite of inner shell spectroscopies to the broadest possible range of user experiments. For the miniXS and XELS instruments, work on this has already begun in the group of G.T. Seidler

from University of Washington. The long working distance spectrometer is adapted from a design like those in use at ESRF, SSRL, CHESS, and elsewhere. See Appendices E and F.

User Community and Demands

By any measure, XAS accounts for around 1/6 of the NSLS user community. XAS and related techniques are routinely performed at 12 of NSLS' 65 beamlines. In 2006, nearly 20% of on-site visitors to NSLS worked at XAS beamlines, over 22% of all NSLS users worked at an XAS beamline., and about 15% of all publications resulting from work at NSLS reported on XAS data. In the period from 2008-2009, users of the beamlines devoted to XAS and related techniques accounted for 20.4% of the total community of ~2200 NSLS users. Subscription rates¹⁹ at XAS beamlines are mostly in excess of 1 and the aggregate subscription rate in that period is nearly 2. NSLS turns XAS users away. XAS beamlines at the other DOE synchrotrons also report subscription rates above 1. The users NSLS XAS beamlines are all potential users of the ISS beamline. The user base for this beamline is enormous.

NSLS XAS users are actively engaged in the development of spectroscopy at NSLS-II. A [technique-based workshop in 2008](#) had over 50 participants. The June 1, 2010 [XAS beamline development workshop](#) had ~40 participants. Access to a high-performance inner shell spectroscopy beamline was identified as a requirement in four of the 2008 NSLS-II Scientific Strategic Planning whitepapers.

Proposal Team Expertise and Experience

Four team members (BR, JB, JW, PN) are beamline scientists at NSLS XAS beamlines. One (AF) is the co-PI of the NSLS Synchrotron Catalysis Consortium. One (LB) has extensive experience in all aspects of optics and beamline design during a distinguished career at NSLS. One (TT) was part of a team that developed an XES spectrometer here at NSLS back in the 90s. Three of the advisory team (BB, MC, SB) are senior members of the synchrotron community and serve on scientific advisory panels for NSLS, BNL, and DOE. One (CG) is the principal scientist at the wiggler-based XAS beamline in Australia. One (GS) is an innovative designer of X-ray spectrometers. Two (SD and WM) are faculty at top-tier universities and outstanding synchrotron scientists. One (SK) is a renowned expert in XAS and author of a recent, important review article on the practice and analysis of XAS. Two (SM and BM) are experts in the application of synchrotron radiation in the field of biogeochemistry. Together we represent the breadth and depth of the spectroscopy community. A one page bio of each Proposal Team member appears at the end of this proposal.

Suggestions for BAT Membership

All local team members as well as Jerry Seidler and Serena DeBeer would be excellent candidates for the BAT.

Appendix A: High heat load beamline optics

The unprecedented brightness and flux of NSLS-II in combination with anticipated developments in optics, detectors, and computing power will lead to many advanced experimental capabilities that are not possible today. Access to these new capabilities and the unique infrastructure envisioned for this new facility will have profound impact on a wide range of scientific disciplines and initiatives and lead to many exciting discoveries in the coming decades.

NSLS-II CD-0 Document

The NSLS-II damping wiggler (DW) offers extraordinary promise in terms of the broad-band, incoherent flux required for inner shell spectroscopy, but also extraordinary challenge in terms of design and development of optics that can accommodate the very high heat load. As we show in this appendix, an ultimate flux of 10^{14} ph/sec in the range of 5 keV to 25 keV with the energy resolution required of an XAS experiment is possible using this source. This ambitious target is an order of magnitude higher than the advertised performance of the world's current highest flux spectroscopy beamline and fully two orders of magnitude higher than most of the world's high-performance spectroscopy beamlines. The promise of NSLS-II has always been to provide new science by advancing synchrotron technology. Here we begin an exploration of how the heat load might be managed to deliver the full potential flux of the DW source.

To deliver the full flux of an NSLS-II wiggler source, beamline optics capable of handling a very high heat load must be developed. This includes windows, filters, mirror, and monochromator. As a baseline for consideration of how this might be done, we can start with the plan developed two years ago for the proposal for an XAS Project Beamline. The heat load management plan developed at that time is presented for reference as Appendix B. Using that plan, we demonstrated how to provide in excess of 10^{13} ph/sec into the experimental hutch while presenting only modest technical and cost risks.

The current situation is somewhat different from the assumptions of two years ago. Most significantly, we had assumed working with canted 3.5 m DW sources. The current DW spec does not allow for canting. However, considering the longer source, a different filtration strategy, and mirror configurations that allow for a larger vertical acceptance, we can, in principle, increase the delivered flux by almost an order of magnitude. This requires several improvements upon what is presented in Appendix B.

1. Remove the first beryllium window. The difficulty of transferring heat adequately out of a thin Be window makes for one of the most serious challenges of designing a high heat load beamline.
2. Design variable thickness filters which can be inserted into or removed from the beam depending on experiment energy and first mirror setting. Filter design is an issue already being pursued by NSLS-II for the XPD Project Beamline. ISS will benefit from these developments.
3. Model and design a high heat load collimating mirror. In 2007, NSLS-II commissioned a study from Accel into the performance of a mirror under high heat load. Those calculations showed that a directly cooled glidcop mirror will certainly suffer large peak slope errors of $\sim 40 \mu\text{rad}$. However, the figure error under heat loads as high as 7 kW remain approximately linear over the entire active surface of the mirror. Although this slope error is substantial, it should be correctable dynamically. Substantial modeling will be required to fully characterize the performance of this high heat load mirror and its impact on beam properties.

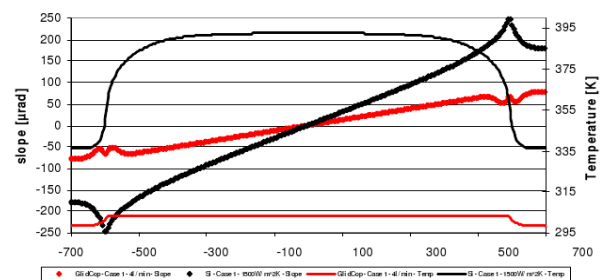


Figure 9: Slope error and temperature on a directly cooled glidcop mirror (red lines) at 7 kW, as calculated by Accel for NSLS-II, August 2007.

4. Model and design a high heat load DCM. This is the area that will require the greatest R&D. As a starting point, we can consider work from SSRL. Their design¹⁵ for a directly cooled, Si(111)

monochromator has been shown to handle up to a 1.1 kW load without significant attenuation of the theoretical transmission. Refinement of the cooling design is certainly a possibility, although experience at the XAS beamline at the Australian synchrotron stresses the importance of designing a low vibration cooling system.

Given that work on filter design is already under way for the XPD beamline and that the 2007 work by Accel suggests an avenue forward for mirror design, we will concentrate here on the issue of DCM design, with an eye towards what is required of the optical configuration to deliver the target flux of 10^{14} ph/sec.

Starting from two existing monochromator crystal designs, the SSRL model¹⁵ which has cooling liquid passing through the body of Si block and the so-called hockey puck which has cooling fins which extend into the cooling liquid, Viswanath Ravindranath from NSLS-II has performed a series of FEA studies of Si(111) under heat load from the DW source. To begin the FEA analysis, beam characteristics for the DW source are computed using Ruben Reinenger's software for the 7 m DW source through a 1 mrad x 0.27 mrad aperture. With the first mirror placed at about 30 m from the source, this aperture collects just over half of the vertical swath and a horizontal swath that will fill a mirror of normal width.

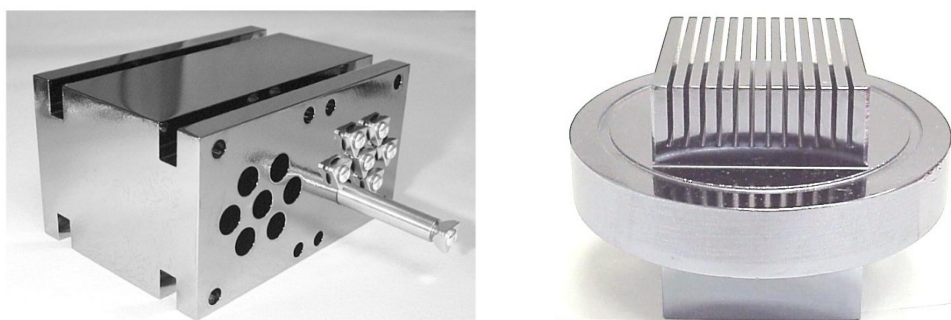


Figure 10: (Left) Photograph of the monochromator from Ref. 15. Note the channels into which LN_2 flow cartridges are inserted. (Right) The so-called hockey-puck design. The diffracting surface is at the bottom in this photo. In operation, the fins extend into a flowing LN_2 bath, providing a large surface area for heat transfer.

This aperture passes 10.5 kW of the total 62.5 kW output of the DW source. This beam is filtered by a 100 μm thick graphite filter, which absorbs 1.6 kW while transmitting $>70\%$ of the flux at 5 keV. A 1.2 m long Pt coated mirror is placed at an angle of 7 mrad, with a critical energy of ~ 9.7 keV. This absorbs 6.5 kW of power, leaving 2.8 kW incident upon the first crystal of the monochromator. This configuration results in a flux out of the monochromator of 10^{14} ph/sec. This, then is the initial condition of the FEA analysis, which was performed for incident angle corresponding to 5 keV and 9 keV operations.

FEA calculations are made using the FEA models created for the two monochromator configurations shown in Fig. 10, 2.8 kW incident power, and the same LN_2 convection cooling model as in Ref. 15. The calculations are made for the cases of 5 keV and 9 keV. These energies are chosen as representative of the range of use of the beamline as as difficult test cases for heat load management. Indeed, the lower energy, 5 keV, represents the most difficult case to be considered for ISS. The peak power densities are 4.25 W/mm^2 at 5 keV and 2.41 W/mm^2 at 9 keV.

The SSRL design is promising. For the 5 keV case, the peak temperature is 172 K and the peak meridional and sagittal slope errors are 40 μrad and 36 μrad . At that energy, the Si(111) Darwin width is 60 μrad . These are large slope errors, but not so large that further consideration is unwarranted. By increasing the number of flow channels and increasing the LN_2 flow rate, the peak slope errors are reduced to 21 μrad and 18 μrad , respectively.

At 9 keV, the situation is improved. For the SSRL design, the peak slope errors are 7 μrad and 9 μrad , compared to a Darwin width of about 30 μrad . The peak temperature is 137 K. The factor-of-2 improvement afforded by the increase in number of channels and flow rate reduces the slope error to around 15% of the Darwin width.

The situation improves substantially upon considering the hockey puck design. With the large surface afforded by the cooling fins, this crystal suffers meridional and sagittal slope errors of $18 \mu\text{rad}$ and $15 \mu\text{rad}$ at 5 keV. At that energy, the peak temperature is 153 K. At 9 keV, the peak slope errors are only $1 \mu\text{rad}$ each with a peak temperature of 125 K.

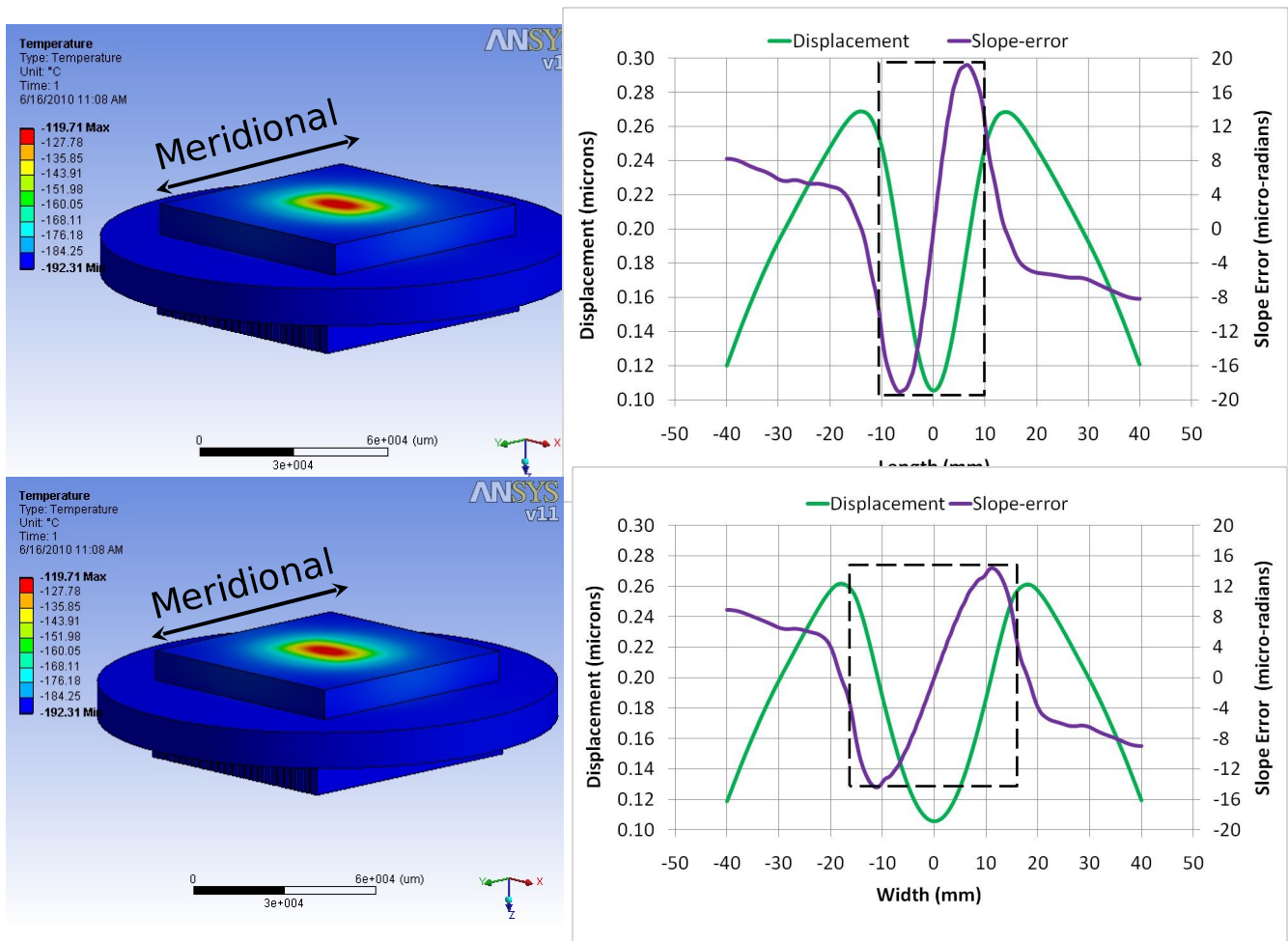


Figure 11: (Top left) Temperature plot of the modeled crystal. Maximum temperature is 153 K. (Bottom left) Displacement plot. (Top right) Meridional displacement and slope error. Peak meridional slope error is $\pm 18 \mu\text{rad}$. (Bottom right) Sagittal displacement and slope error. Peak sagittal slope error is $\pm 15 \mu\text{rad}$.

The results at 5 keV for the hockey puck are shown in Fig. 11. Even with this level of slope error, the Si(111) crystal is highly transmitting, although there are significant effects of energy and positional spread of the beam that would have an impact on use of the beam. By 9 keV, the slope errors are quite small even despite the high heat load of 2.8 kW.

These results are extremely encouraging although clearly this is an incomplete analysis. This FEA analysis suggests that the directly cooled hockey puck crystal can support the 2.8 kW load required to deliver a flux of 10^{14} ph/sec. The situation is somewhat worse at the lower energy. But even there, these results are encouraging. At the very least, the heat load can be reduced by additional filtration and flux well in excess of 10^{13} ph/sec is possible. Ray tracing to determine the effect of the slope error on the performance of the beamline is warranted. Given the modest requirements of ISS on source brightness, the impact of the slope errors at lower energy might be tolerable.

Appendix B: Heat Load Management at the Damping-Wiggler XAS Beamline

Paul Northrup (March 7, 2008)

[Note: This section was prepared for presentation to the March 2008 meeting of the NSLS-II EFAC and was submitted as supporting documentation for the XAS Project Beamline proposal. It is presented here verbatim except for two sections which are not relevant to the current proposal. Although some details of the damping wiggler design, most importantly the ability to cant 3.5 m source, have changed in the intervening years, this remains useful as a template for designing a beamline to work on the current DW design.]

Summary: This document was prepared as a supplement to the Preliminary Design Report (PDR) in response to reviewer concerns of the manageability of the high power delivered by the NSLS-II Damping Wiggler (DW) insertion device. The DW was chosen as the best source for the Project X-ray absorption spectroscopy (XAS) beamline based on its properties of high flux, broad continuous energy range, and non-coherent nature. A divide-and-conquer approach was employed to distribute heatload over different beamline components. Initial considerations of heatload assumed worst-case configurations in an effort to make the most robust design possible. However, it soon became clear that several components could not tolerate the full brunt of unfiltered power being considered for a 7m-long DW.

Therefore the calculations presented in this document were undertaken to determine realistic heat loads on beamline components in the configurations expected under actual use. As a result, heatloads on individual components are shown to be well within the desired tolerances. Further, it will not be necessary to compromise beamline performance or flux in order to manage heat load.

Beamline requirements, parameter limits and assumptions: This document supplements the PDR, last revised January 2008. The goal of the XAS beamline is to deliver very high flux over a wide continuous energy range, while maintaining excellent stability and repeatability of beam position and energy calibration. Energy range is limited on the high end by the insertion device and on the low end by the Be window and necessary filtration. The DW source is assumed to be a 3.5m-long DW90 device (37 poles, $K=15.2$) in the upstream canted position. This follows the design decision to employ a canted geometry from day one rather than two in-line segments that would be canted at a later time.

The acceptance angles for beamline optics determine the maximum fraction of the DW fan that will impact components. Vertical acceptance is calculated for a collimating mirror of variable angle (depending on configuration as described below) assuming a length of 1.5 m (1.45 m reflective surface) and a position of 33.65 m from the center of the DW. These positions are based on the shieldwall positions as of January 2008 PDR revision, and use of the upstream (outboard) canted wiggler segment allowing 0.5 m for the canting bend. Horizontal acceptance is limited by the 1.0 mrad design maximum (based largely on front end mask limitations), and also by effective acceptance of the monochromator. This is a function of the effect of horizontal divergence on the diffraction angle, relative to the rocking curve of the crystal at a given energy. For example the maximum vertical angular deviation for 1 mrad of horizontal acceptance is 6 μ rad. This becomes a significant consideration at higher energies and for higher-energy-resolution experiments, where the monochromator rocking curve is less than 6 μ rad.

Carbon foil array filters and the standard 0.25mm Be window are positioned at 31 m and 32 m, respectively, and the monochromator at 35 m.

Selected configurations: The following operational configurations were considered. These were chosen as the smallest set of fixed repeatable configurations to best serve experimental needs, cover the energy range, maintain harmonic-rejection, and distribute heat load. Possible adjustments to filter thicknesses, mirror angles, and coatings will shift these energy ranges and acceptances, but the current set is also optimized for experimental needs. If necessary, additional configurations could be included for even closer heatload management. Note that collimating mirror angle effectively determines maximum vertical acceptance.

Configuration	Filters	VCM angle/coating	Energy range	Angular acceptance (horiz x vert)
1	250 μm C	3.15 mrad, Si	5.7-9.8 keV	1.0 x 0.136 mrad
2	500 μm C	2.0 mrad, Si	7-15.2 keV	1.0 x 0.086 mrad
3	5 mm C	3.15 mrad, Pt	14.4-26 keV	1.0 x 0.136 mrad
4	7 mm C	2.0 mrad, Pt	17-35 keV	1.0 x 0.086 mrad
5	5 mm C + 110 μm Ni	1.6 mrad, Pt	35-50 keV	0.3 x 0.069 mrad

Table 1: Optical configurations used in different energy ranges.

Be window and pre-filters: The Be window is required as a vacuum-isolation measure between beamline components and the front end. A windowless configuration would have much more stringent beamline vacuum requirements, and is not recommended where the monochromator is direct-cooled with LN₂ (a possible design here) or the collimating mirror is direct-water-cooled (as it is here). The standard Be window is 250 microns thick, 10 mm high, and as wide as necessary for the maximum fan of beam used.

Protection of the Be window from the lowest-energy radiation requires a graphite pre-filter, in an array of increasing-thickness foils. This is based on the expected requirement to keep the Be temperature below 100C; above that temperature the stress of repeated thermal cycling may eventually weaken the window. Interestingly, this component appears to be the most power-limiting element of the XAS beamline. The combined absorption of the pre-filter and the Be window effectively set the minimum usable energy for the beamline.

Initial FEA calculations by Accel (provided in report of September 2007 and supplement October 2007) demonstrated that for a vertical acceptance of up to 0.15 mrad (4.65 mm), a 10 mm high Be window would not perform adequately using any reasonable pre-filter thickness. However, a 5 mm high window would maintain an acceptable temperature provided its absorbed heat load was kept below 72 W. Using this approximation, for what is a complex function of total power, power density, and footprint, the minimum pre-filter thickness was re-calculated for the selected operational configurations. The result is 250 microns of graphite as a pre-filter, and a minimum usable photon energy of approximately 5.7 keV. There is still significant flux below that energy, but the slope of flux vs energy is too great for reasonable normalization. These parameters will continue to be refined as beamline design and shieldwall configuration evolve. Another round of FEA calculations is required.

Using a window height that is barely larger than the beam footprint (5 mm compared with 4.65 mm) will require careful alignment as well as measures to protect the window frame and braze from direct beam. This can be best accomplished by placing the Be window on the downstream end of the in-vacuum Bremsstrahlung collimator at 30 m and providing a very limited vertical adjustment.

Note that changing Be thickness does not offer any advantages. Thicker Be will conduct heat better, thus cooling more efficiently, but will absorb approximately an equivalent amount more power. Thinner Be is similarly indifferent, and is less robust than the standard thickness. The other geometric option is to place the window at an angle to the beam, by rotating in the horizontal plane, to thus spread the power density across a greater width of Be. Although this increases absorption, using a thinner window would result in a marginal gain of 5-10% in heat load capacity. That is not sufficient to justify the added complexity and risk at this phase of design.

Depending on cooling-water temperatures (current design is considering raising this to 85 F), and new FEA results, it will likely be necessary to employ a colder cooling loop for just the Be window.

The pre-filter design of choice is similar to that employed at NSLS Beamline X25, and consists of an array of graphite foils. These are of increasing thickness, from 5 to 100 microns each, and are cooled radiatively. The power is indirectly captured by water-cooling of the filter holder frames and by surrounding the array with a

cooled shielding enclosure. Further “baffles” between the foils and on each end, having openings just larger than the beam size, limit thermal radiation and scatter that may otherwise heat other components.

Retractable filters: A sequential array of optional additional filters will be used for configurations above the lowest energy range (Table Error: Reference source not found). These thicker graphite filters absorb more of the lower energy power, and bear more of the heatload burden for configurations where the collimating mirror absorbs less. Thus the heatload delivered to the monochromator remains tolerable.

The filter sequence would start at 250 microns graphite and include up to 7 mm net thickness. For the highest energy ranges, filters composed of heavier elements such as Si or Ni (freestanding or in composite with graphite) could be added. Heatloads for operations above 35 keV are well below concern due to the limited acceptance, but power density remains an important issue.

FEA calculations will be needed for these filters as well, but such filters are not expected to be pushing the limits of the technology. It may be necessary for the first one in the series to be constructed from more than one layer, akin to the pre-filter design.

Collimating mirror: The collimating mirror bears most of the heatload at lower energies and corresponding higher incidence angles. Initial FEA by Accel showed that by using direct cooling one could effectively dissipate approximately 2.5 kW, and fully correct for the thermal distortion by adjusting the bend. However, a heatload of 4 kW produced a small slope error (0.1 μ rad) even after compensation by adjusting the bend. Indirect (side) cooling of the mirror was unacceptable even at less than 2.5 kW. Therefore it is reasonable to make the design decision to use direct cooling, and to set a maximum operational heatload of 2.5 kW.

Further FEA calculations will be needed to more closely quantify thermal distortion both along and across the reflecting surface, for the appropriate set of configurations. Realistic estimates of surface roughness and coating thickness will also need to be incorporated. Accel’s calculations considered over-illuminating the reflective surface so as to avoid boundary effects; in practical application this portion of the mirror (and the fate of its portion of the reflected beam) must be accounted for.

Monochromator: The most critical component for heatload concerns is clearly the monochromator. Thermal distortion of the first crystal affects throughput (flux), focusing performance (angular divergence), and stability (over angular changes with energy). Such distortion is modeled by FEA and usually quantified on the basis of maximum slope error.

A survey of existing facilities worldwide indicated that first-crystal heatloads of up to 700 W can be effectively managed using cryo-cooled Si(111). Designs differ: most are direct-cooled, which is more difficult to implement and to maintain, while some are indirect-cooled (for example the Australian Synchrotron XAS wiggler beamline). FEA by Accel for the NSLS-II beamline indicated that a direct-cooled monochromator could handle total heatloads up to 1.3 kW with acceptable slope error of less than 4 μ rad. An indirect-cooled design was shown to handle up to approximately 700 W with similar distortion. These were calculated for 23 degrees theta (the worst-case geometry, for 5 keV monochromatic beam), although they used pre-filter thicknesses which were not realistic for actual operation. Crystal geometry used for the indirect-cooled model was a large rectangular block as described in the Accel monochromator design document (and employed at the Australian Synchrotron); the same geometry was used for the direct-cooled model but a modified set of thermal contact parameters was employed.

In-house preliminary FEA (conducted by V. Ravindranath) used the direct-cooled “hockey puck” design employed at several beamlines. These calculations did not yet include any filters or mirrors, but optimized crystal dimensions and considered the benefits of under-cooling the LN2. Results indicated that for 0.15 x 0.25 mrad acceptance (1.8 kW from an unfiltered 7m DW100 source) the maximum slope error is 23 μ rad. Extrapolating from these results indicated that about 1.2 kW would be the maximum tolerable heatload for a 0.15 x 1.0 mrad footprint.

Based on these early results, the current design includes provisions for direct cooling of the first crystal, with the expectation that indirect cooling would be the preferred option if more detailed study showed it feasible. A

maximum operational heatload is set at 700 W. This is achievable without compromising beamline performance based on operational configurations in Table 1 and a canted 3.5 m DW90 source. Further FEA is under way utilizing more appropriate filter conditions and crystal geometries. These constraints are, however, only qualitative boundaries: greater thermal distortion may be acceptable for some applications where performance (energy resolution, focus) is less critical, and even stricter requirements may be applicable to the most demanding of experiments.

Slope error is only one aspect of thermal distortion to be considered. A rigorous analysis will combine FEA and ray-tracing in a 3D treatment of the monochromator. Thermal distortion will include energy distribution across the beam footprint, energy-dependent penetration depth and power absorbed in the 3D solid, 2D slope error across the beam footprint, and lattice (d-spacing) change throughout the solid. Ray-tracing will utilize the fully-characterized solid with respect to the 3D diffracting volume, including such aspects as angular mis-orientation, surface distortion, d-spacing mismatch, tune between crystals, and rocking-curve width.

Predicted maximum heat loads: The following table shows realistic expected heat loads on the various components in the five configurations described above (Table 1). Filters absorb a higher fraction when working at higher energies, while the collimating mirror absorbs a larger share at lower energies. The effect of reduced angular acceptance at higher energies is shown in the total power column. All values are below the maximum allowed heatloads as described in the sections above, and represent the highest heatloads theoretically possible for each configuration.

Configuration	Total power	Filters	Be window	VCM	Mono
1 (5.7-9.8 keV)	3624 W	693 W	69 W	2363 W	499 W, Si(111)
2 (7-15.2 keV)	2416 W	599 W	33 W	1139 W	643 W, Si(111)
3 (14.4-26 keV)	3624 W	2222 W	15 W	728 W	661 W, Si(111)
4 (17-35 keV)	2416 W	1606 W	8 W	189 W	613 W, Si(111)
5 (35-50 keV)	607 W	529 W	1 W	18 W	57 W, Si(333)
Maximum allowed load			72 W	2500 W	700 W

Table 2: Heatloads on various heat-bearing optical components in the various configurations.

Considerations for achieving higher energy resolution: For applications requiring higher energy resolution, typical strategy elsewhere is to use an alternate higher-resolution monochromator crystal pair. The strategy developed here, in light of the large heatload issue, is unique. Rather than relying on an alternate crystal set (e.g. Si311) in the high heatload monochromator, the DW XAS beamline design employs a Si(111) primary monochromator to bear the brunt of the heat load and a synchronized second monochromator in series to refine the energy to higher resolution. In that way, greater thermal distortion is tolerated in the wider-bandpass Si(111) crystals, while greater throughput is achieved with the undistorted high-resolution crystals. This also allows selection of appropriate high-resolution crystal materials without regard to their thermal tolerance.

Crystals with narrower bandpass naturally have lower tolerance for thermal distortion. Performance calculations were made comparing throughput of Si(311) in the high-heatload monochromator versus Si(111) followed by Si(311). Taking into account a reasonable approximation of thermal distortion (as discussed above), these calculations showed that the two-monochromator design produced approximately 40 times higher throughput than would Si(311) alone.

Scatter shielding: For such a high-power beamline, even scattered radiation may transfer significant heat to components not in the direct beampath. This requires the addition of water-cooled shielding, baffles, and masks around and between white beam components. Such shielding will surround the pre-filters, retractable filter assemblies, and Be window. An additional design feature of the collimating mirror will be a shielding shroud

over the sides and above the face of the mirror (dubbed the “Conestoga wagon”), to keep scattered radiation from heating the enclosure and the positioning and bending mechanism components.

Particular attention will be paid to scatter-shielding within the monochromator, both for thermal load and for monochromatic beam quality. Both crystals will be LN2-cooled, to minimize thermal effects from scatter, while water-cooled shielding will protect other components and mechanisms. The feasibility of a “tracking mask” between the first and second crystals will be investigated.

Changes in configuration: Since these calculations were initiated, there have been some changes to shieldwall position and beamline component locations. These refinements are expected to continue, especially at this early design stage, and will impact such parameters as power density and angular acceptance. Design changes will be monitored, and heatloads recalculated periodically, but the values presented here should remain substantially correct (within 10%). In addition, as the larger design issues become settled, beamline component design can then be optimized to deliver the best possible performance. This will include such aspects as filter thicknesses, mirror angles, and component cooling schemes.

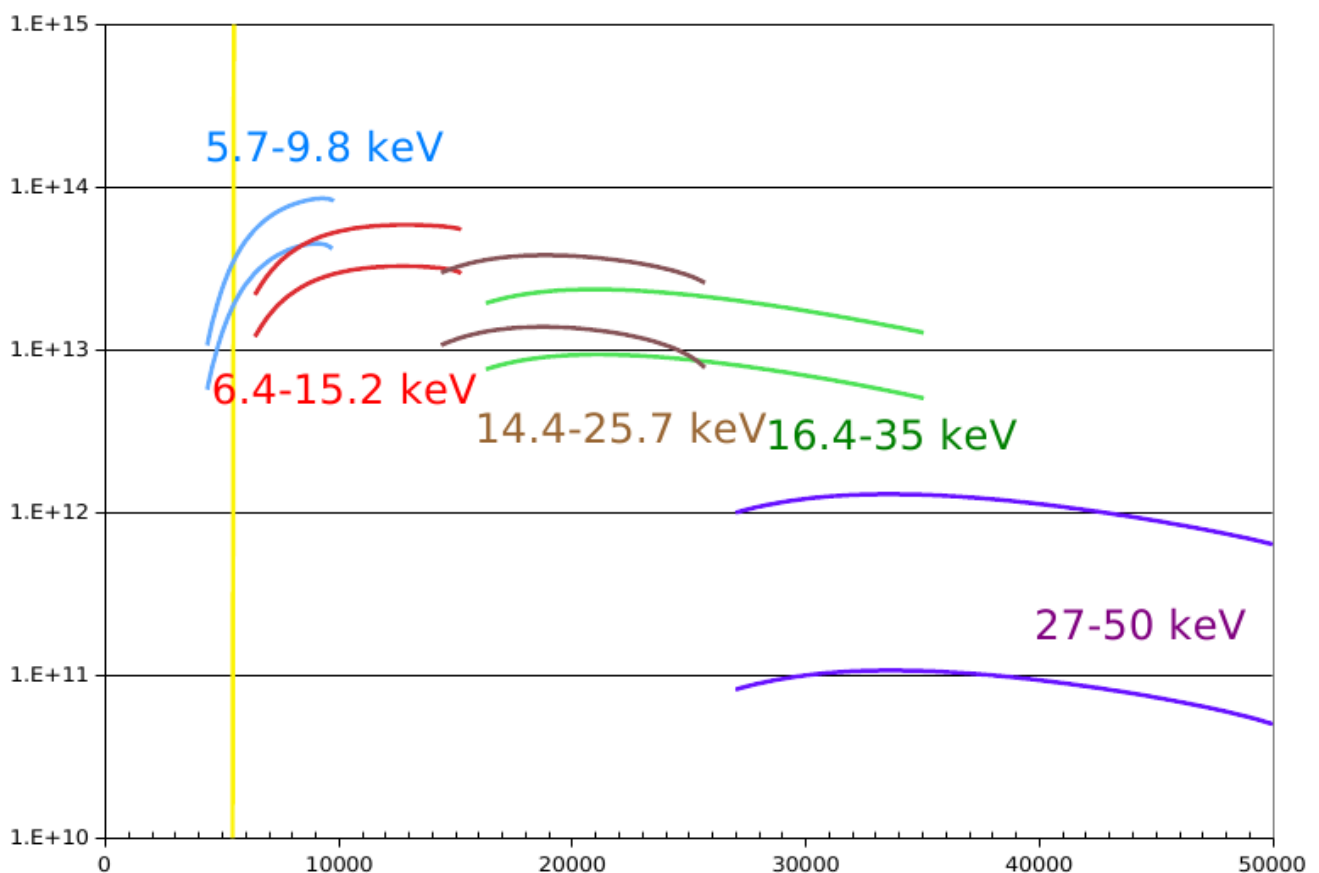


Figure 12: Flux using the various configurations described in this appendix and using the canted 3.5 m DW sources that were assumed for the 2008 XAS Project Beamline proposal. The margins represent a spread of delivered flux based on optimistic and pessimistic assumptions about thermal distortions on the VCM and DCM.

Appendix C: High energy resolution inner shell spectrometry

A typical XAS measurement made using an energy discriminating solid state detector is capable of resolving the α fluorescence line of transition metal and heavier atoms from the β line. However the energy resolution of any energy discriminating detector is inadequate to resolve any structure within those fluorescence lines. This is shown for Mn in Fig. 13. The ultimate energy resolution of an XAS experiment is determined by the bandpass of the x-ray monochromator and the natural Lorentzian width that results from finite lifetime of the core-hole. With a silicon monochromator and in the energy range of hard X-ray XAS beamline, the lifetime broadening of the core-hole exceeds the monochromator bandpass.⁸ The natural linewidth can be reduced by better defining the observed final-state energy of the electron-core hole pair decay channel.^{10,11} We are proposing the implementation of two spectrometers at the ISS beamline.

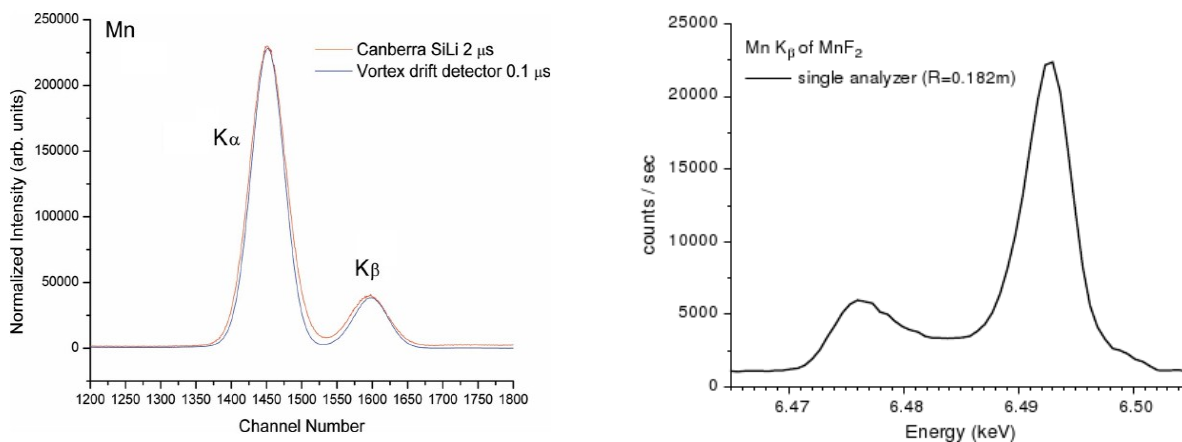


Figure 13: (Left) The Mn $K\alpha$ and $K\beta$ fluorescence lines measured with a silicon drift detector with ~ 220 eV energy resolution. (Right) The Mn $K\beta$ line measured with a crystal analyzer with ~ 0.5 eV resolution. The $K\beta_{1,3}$ and $K\beta'$ lines are clearly resolved.

Long working distance XES spectrometer

The long working distance XES spectrometer²⁰ works by placing one or more bent crystal analyzers on Rowland circles. With more than one analyzer, the Rowland circles are made to intersect at two points, as shown in the inset of Fig. 14. The sample sits at one intersection and a point detector sits at the other. The working distance – the separation between sample and analyzer crystals – is typically around 1 m. A spectrometer of this sort is the principal instrument for the XAS/XES program at ESRF ID26. Other such spectrometers are in use at SSRL 6-2, CHESS Station C1, and elsewhere. One of the earliest such instruments was developed here at NSLS.⁹ The very high flux of ISS offers the enticing promise of making XES and high-resolution XANES measurements quick and routine, particularly if combined with a spectrometer with a far larger number of analyzer elements.

The XES spectrum is measured by fixing the incident beam energy and scanning the spectrometer through a bandpass wide enough to cover an entire fluorescence line, typically a few 10s of eV as shown in Fig. 13. This energy scan is accomplished by translating the crystal elements and the detector vertically, thus changing the wavelength for which the Rowland circles shown in Fig. 14 overlap. A high-resolution XANES scan is then measured by placing the spectrometer at some feature of the XES spectrum, for instance the peak of the $K\beta_{1,3}$ peak, and varying the incident energy as in a normal XAS scan. In this way, the broadening due to the core-hole lifetime is reduced, resulting in spectra like the one shown in Fig. 5 on page 4 on the main body of the proposal.

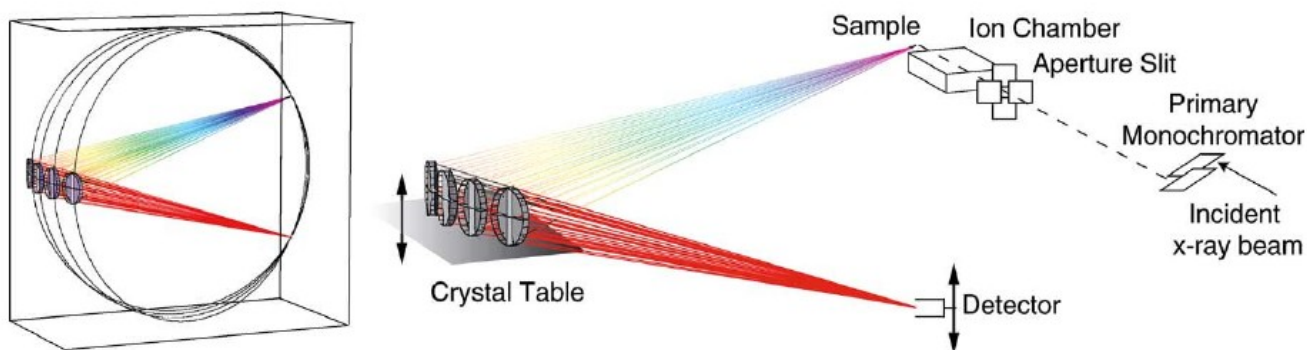


Figure 14: Experimental set up of the long working distance spectrometer. The arrows indicate the motion of the components during an XES spectrum. The inset shows the orientation of the Rowland circles for the four analyzer crystals shown in the schematic. Figure from Ref. 20.

High-resolution XANES is applicable to virtually every XAS experiment in every field that uses XAS. As stated in the main body of this proposal, a common use of XAS is to determine valence and chemical state via the near-edge structure. Because of the core-hole broadening, this is often challenging. For example, the various forms of iron oxide and iron oxyhydroxide are quite similar in their XANES. In a mixed phase system, quantification of phases by a linear combination analysis is often uncertain due to the core-hole broadening. Higher resolution XANES spectra, in many cases, removes ambiguity from this analysis, thus improving quantification of phases. For higher energy edges, uranium L_3 for example, the core-hole broadening is quite large relative to the valence shift observed between oxidized and partially reduced forms of uranium, thus impeding the ability to quantify a partially reduced system. Again, high resolution XANES is a great benefit.

Although the effect of reducing the broadening is most pronounced near the edge, this spectrometer can be put to very good use for a variety of exotic EXAFS measurements. In Ref. 26, the authors show a EXAFS spectrum for the mixed-spin, iron cyanide Prussian Blue. By tuning the spectrometer to carefully chosen points in the XES, XAS spectra dominated by one spin state or the other can be measured. The fine resolution of spectrometer allows measurement of specific fluorescence lines even when other elements in the sample fluoresce at nearby energies. In this way, EXAFS can be extended²¹ beyond an intervening edge. The XES spectrometer can also be used in the manner of the typical energy dispersive detector to measure XAS spectrum on a minority element can be measured in the presence of majority component with similar fluorescence energy, albeit with the ability to reject the majority signal far more efficiently than with the energy dispersive detector.

Long working distance spectrometer used for XELS

The XELS spectrometer is described in detail in Appendix D and operates similarly to the long working distance XES spectrometer. Instead of tuning the analyzer crystals to an energy associated with a particular fluorescence line, they are tuned to some high energy. In the schematic of the XELS process shown in Fig. 1, the analyzers are tuned to 10 keV. A soft X-ray edge is thus measured by scanning the incident beam through an energy range above the tuning energy of the fixed analyzer crystals. On top a large Compton background, the energy loss features associated with soft X-ray edges are seen. This is seen in Fig. 15 which shows the XELS as measured by the LERIX spectrometer²² at APS beamline 20ID. This spectrometer is similar to the long working distance spectrometer proposed for ISS except that the analyzer crystals are arranged in an arc around the sample such that XELS is measured for a large range of momentum transfer. In Fig. 15, the Compton peak is seen dispersing in energy as the momentum transfer is increased. On top of that, the much smaller XELS features are seen. In this experiment,²³ a titanium-bearing pyrochlore was measured by making fine scans through the regions indicated in Fig. 15. The data for the O K, Ti $L_{2,3}$, and Ti M are shown in Fig. 16.

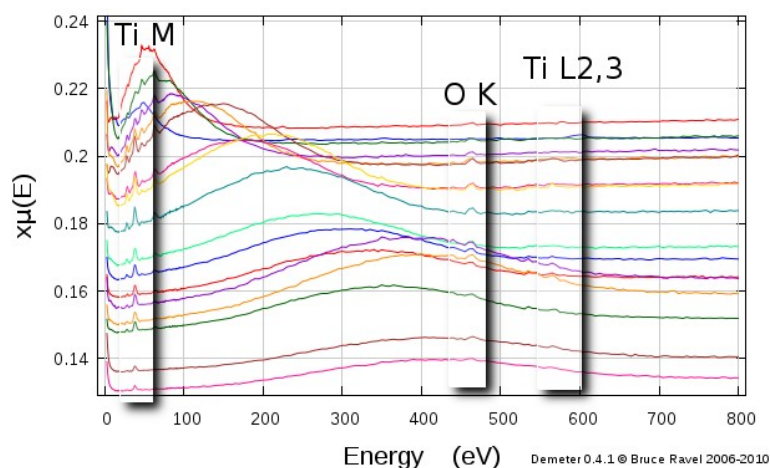


Figure 15: Momentum transfer dependent XELS measured on a titanium pyrochlore with the LERIX²² instrument. Note the broad Compton peak dispersing in energy as the momentum transfer is changed. The soft X-ray edge regions are highlighted.

With an estimated flux on the sample of about 5×10^{12} ph/sec, these two figures represent about a day of beamtime at APS 20ID. With an order of magnitude high flux and a spectrometer with a larger number of scattering elements, ISS makes this sort of measurement much more routine.

The applicability of XELS extends anywhere that soft X-ray spectroscopy is currently performed. Because it uses a hard X-ray incident beam, it is an unambiguously bulk-sensitive probe, making it a useful complement to conventional soft X-ray spectroscopy. The hard x-ray probe also makes this measurement compatible with any sample environment designed for a conventional XAS experiment, making it possible to combine XAS and XELS in any kind of *in situ* or *operando* experiment.

Short working distance XES spectrometer (miniXS)

The aspect of the long working distance spectrometer that limits the data collection rate are the total collection solid angle (for weak XES) or the motor motion times (for strong signals). The use of a position sensitive detector has led to interesting trade-offs in this field, with vastly improved measurement times for very high-resolution studies²⁴ and interesting options to convert focusing optics to wider-band dispersive optics by working off-circle.²⁵ Another variant which leads to a high-throughput dispersive spectrometer is the short working distance, or miniXS, spectrometers.¹ In the latest iteration of these instruments (see Fig. 17), which will soon be a standard part of the 20-ID XAS microprobe endstation at 20-ID, several flat dispersing elements are placed onto a Rowland circle geometry with only ~8 cm diameter. The active region of each crystal subtends a collection solid angle comparable to one or two typical spherically bent crystal analyzers, resulting in net collection solid angles comparable to that for large arrays of spherically bent crystal analyzers in an inexpensive and versatile framework. Due to the Rowland-like configuration, each diffracting element sends the same analyzed energy bandwidth through an appropriately placed exit aperture. When the crystals are properly placed, as per solution of the relevant inverse problem, the resulting dispersed spectrum from each crystal will perfectly fill the areal detector with no overlaps (see Fig. 18, which comes from a high-pressure DAC study using a similar instrument).

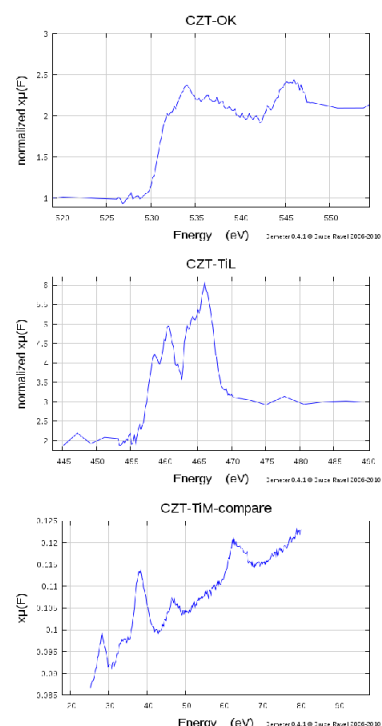


Figure 16: Bulk absorption spectra measured by XELS for O K, Ti L2,3, and Ti M for the titanium pyrochlore.

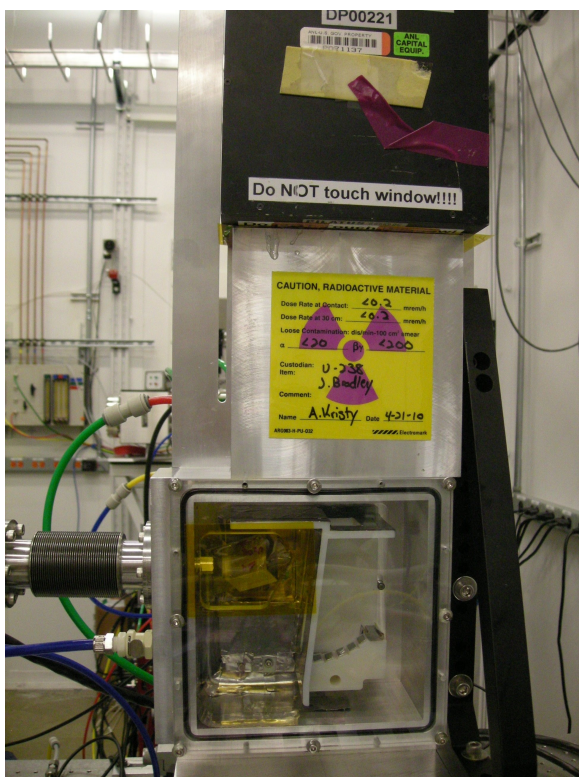


Figure 17: The miniXS spectrometer. Photo courtesy of Jerry Seidler, University of Washington.

In Fig. 17, which shows the miniXS instrument configured to perform U M-edge XES, the beam is incident from the back of the spectrometer. The emitted radiation which strikes the small (~ 1 cm) crystals on the right hand side of the white, plastic optics holder is Bragg-scattered and analyzed, resulting in several copies of the same dispersed spectrum on the [Pilatus 100K](#) camera, placed ~ 14 cm above the exit aperture for the instrument. The sample is mounted behind the yellow polyimide window, which allows passage of x-rays for conventional XAS. An example of

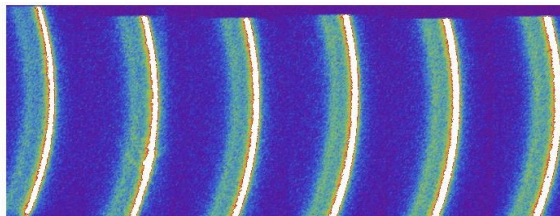


Figure 18: XES for Fe_2O_3 as measured using the miniXS instrument. The bright stripes are the Fe $K\beta_{1,3}$ peak as imaged by each crystal. The greenish bands to the right of each bright stripe are the weaker, lower energy $K\beta'$ lines.

resulting XES image is shown in Fig. 18. Note that the separation between the sample and the crystal carriage is quite large enough to accommodate a specialized sample environment for temperature controlled or *in situ* experiments.

Specialized image processing is required to convert these images to XES spectra. First elastic scattering is exposed to the areal detector through the energy range of the fluorescence lines. This defines the association of

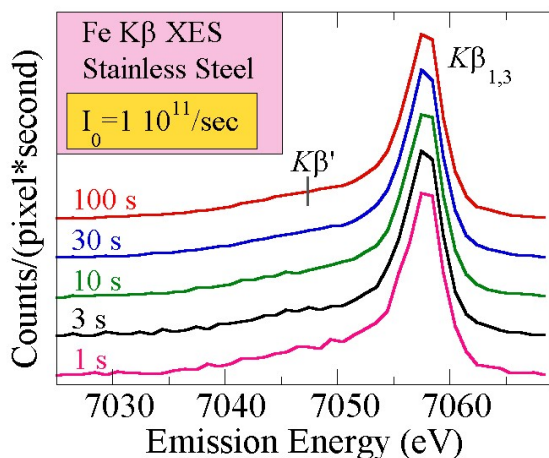


Figure 19: XES spectra from stainless steel after processing as described in the text.

each pixel in the detector to emitted energy. Then the signals from each pixel associated with the same energy are binned to yield spectra like those shown in Fig. 19. With a relatively modest flux of 10^{11} ph/sec from APS 16ID, a decent XES spectrum can be collected in 1 sec. After about two minutes, the statistics are good enough to resolve the very small $K\beta'$ peak. With the much superior flux of the ISS beamline, this counting time is substantially reduced for concentrated samples and dilute samples become easier.

With efficiencies gained by measuring both dispersively and redundantly and by using the larger [Pilatus 300K](#), the miniXS instrument opens up a range of experimental possibilities. The XES measurement is fast enough to consider μ XES mapping of a heterogeneous sample. The full RXES²⁶ plane, that is the measure of XES as a function of incident energy through an

absorption edge, can be measured efficiently. Finally, the fast XES measurement allows for time-resolved XES, as described in the main body of the proposal.

Appendix D: XELS end station at the ISS beamline

Gerald T. Seidler (University of Washington)

Given the rapidly diversifying application of x-ray Raman scattering (*i.e.*, nonresonant inelastic x-ray scattering from semi-core and core level initial states), we propose to construct a high throughput X-ray Scattering (XRS) spectrometer to serve the users of NSLS-II. This technique is especially well-suited to NSLS-II, thanks to the anticipated extremely high brilliance of the new light source: XRS is a photon-starved technique in all but the simplest experiments. Either of two directions may then be reasonably pursued. First, one may aim at the absolute highest throughput while retaining the option of ‘good enough’ energy resolution to preserve much, but admittedly not all, of the information in the pre- and near-edge region. This would mean, for example, having net energy resolution (for monochromator plus spectrometer) of ~ 0.5 eV for studies of the near-edge region but of only $\sim 1.5 - 2$ eV for studies of the extended region. Second, one may instead focus exclusively on the problem of achieving near-edge spectroscopy limited essentially by the core-hole lifetimes of the target species. For the $1s$ shell of light elements and the $2p$ shells of the 3d transition metals, this means an energy resolution of $\sim 0.1-0.2$ eV.

While it is possible to combine these two options in the same spectrometer²⁷, to do so runs into some fundamental limitations which compromise the performance of the lower-resolution, high-throughput option. Most obviously, the low-resolution and high-resolution instruments are best sited at, respectively, wiggler and undulator sources; the wiggler provides optimal flux but insufficient collimation for effective use of the monochromators needed for high-resolution studies, and conversely for the undulator source. Also, the high-resolution instrument requires the use of ‘dispersion compensation’ with x-ray sensitive area detectors^{24,28} to reach the desired energy resolution with a 1-m diameter Rowland circle instrument. The resulting coupled constraints on the area detector location(s) and the density and arrangement of large arrays of spherically bent crystal analyzers provide a substantial barrier to achieving the highest throughput for the lower-energy resolution (*i.e.*, 0.5 eV – 1.5 eV) option. We admit that an additional complication arises for applications requiring extremely small spot sizes, mainly Mbar-pressure DAC studies: such studies would benefit from a wiggler source for flux, but require an undulator to have fine enough collimation for the needed focus. Hence, it is clearly the case that one instrument, and in fact one beamline, cannot optimally satisfy both useful goals.

In the present case, where we are operating a wiggler beamline, we have chosen to pursue only the lower-resolution, higher-throughput direction. We believe that such an instrument at NSLS-2 will effectively serve numerous scientific communities, as we have summarized in the scientific portion of this BDP. To this end, we propose to build a massively multi-analyzer IXS spectrometer, which we have named the **X-ray Energy Loss Spectrometer** (XELS), to emphasize the conceptual similarities between nonresonant IXS and EELS, and also to indicate that the spectrometer’s applications will span valence, semicore, and core level initial states – *i.e.*, an XRS spectrometer geared for spectroscopic studies.

We now outline the projected spectrometer design and performance targets. We say ‘projected’ due to long timeline until proposed completion of the ISS beamline together with the lessons which can be learned in the interim from the several ongoing projects to modify or commission large XRS spectrometer at the APS (LERIX-1B and LERIX-2), the ESRF (ID-16 and the planned ID-16 upgrade), and SSRL (Bergmann’s ~ 100 analyzer system). Members of the ISS team are involved in the APS efforts and will remain in close contact with the relevant scientists at the other facilities as the various instruments are designed, constructed, and commissioned. We do not doubt that unforeseen challenges, and opportunities, will occur in the construction of such instruments in the next few years; the ISS team will be well-placed to learn from these positive and negative experiences, and to incorporate that information into the final XELS design.

That being said, our starting point is as follows:

- A. **Spherically bent crystal analyzers:** Si 660 analyzers will be used. These will be strain relieved 10 cm diameter optics with 1-m radius of curvature. As shown in figure X, such optics have been successfully deployed at ID-16 of the ESRF, and have demonstrated an 0.41 eV energy bandpass (the resolution in

that figure is broadened by the 200 meV monochromator bandpass). When combined with the energy refining monochromator at 10 keV the resulting net energy resolution will be 0.5 eV.

- B. **Analyzer alignment modules:** Following the ID16 ESRF experience, the methods of the SSRL instrument, and the plans for the LERIX-1B and LERIX-2 instruments, each spherically bent crystal analyzer (SBCA) will be controlled on two tilt axes and one linear translator (toward and away from the center of the Rowland circle). This allows the maximum freedom for distributing the analyzer reflections between different detection channels (i.e., overlapping or non-overlapping images on area detectors) or for modifying the overall instrument ray-tracing to allow larger clearances near the sample location for special sample environmental apparatus.
- C. **Spectrometer superstructure:** There are several different approaches to the placement of analyzer modules so as to obtain high coverage while retaining flexibility in analyzer positioning – in fact, the several LERIX instruments, the ESRF ID16 instrument and planned upgrade, and the SSRL instrument all take reasonable but different approaches to this problem. Given that the main goal of the XELS instrument at ISS are optimum throughput and given that the analyzers, being relatively low energy resolution (i.e., wide rocking curves), will be fairly easy to align as long as the wafer mis-cut transferred to the final analyzer is well-characterized, we favor a brute-force approach. Specifically, we will work along the lines of the planned LERIX-2 instrument at the Advanced Photon Source. A partial 2.5 m diameter geodesic-like dome will be constructed with numerous fittings for high-tolerance kinematic mounting of units of three to 14 analyzer modules within ± 30 degrees of the vertical scattering plane when at $2\theta = 90$ deg and farther out of the scattering plane when near the forward and backward scattering geometries.
- D. **Detectors:** Barring significant new developments in low-noise x-ray area detectors, three to four of the Pilatus100k detectors (or a custom assembly thereof) will be used. These will be augmented by a multiple stages of spatial filtering to minimize stray scatter, such as is required in any such instrument. While the spatial degrees of freedom may, in some cases, be used for filtering of the ‘imaged’ scattering from sample chamber walls, more often we will define ROI’s on the face of the area detector and then effectively simplify the data processing down to an array of ‘one-pixel’ detectors. The targeted energy resolution does not require the use of dispersion compensation.
- E. **Overall ray-tracing:** Some details are still under development. Briefly, neighboring analyzers at similar q will typically share a small detector region, and will often, but not always, share the same Rowland circle. The instrument will be configured to occasionally move between two different Bragg angles: 88.5 deg for ‘typical’ operation and 87 deg as a ‘maximum clearance’ mode when required by several users with environmental chambers which must be long in the direction perpendicular to the vertical scattering plane.
- F. **Collection solid angle:** We target a final coverage of 20% of the upper 2π steradian half-sphere; given the polarization dependence of XRS, this is closer to 40% of the useful scattered radiation at typical values of q . Such coverage requires ~ 200 spherically bent crystal analyzers. Note that XELS is inherently a modular system. Consequently, the instrument can be built and commissioned with a much smaller number of analyzers, i.e., ~ 50 SBCA, in assemblies of ~ 10 SBCA which can be re-positioned and re-tuned as needed. Final scale-up to fill the spectrometer frame can then follow, building on the results of the beta-version spectrometer.
- G. **Primary and secondary monochromator, and net energy resolution:** The heat-bearing principal monochromator combined with the energy refining monochromator provide adequate energy resolution for calibration and operation of the XELS end station.
- H. **Focusing optics:** A secondary source aperture and Kirkpatrick-Baez mirrors will be used to focus to a ~ 50 μm spot. If required, several analyzers at the upstream end of the XELS instrument can be removed to accommodate the KB optics.

- I. **User-ready support equipment:** Custom cryostats, furnaces, and He-filled or vacuum-compatible sample chambers will be available for users. A motorized 2-axis goniometer with high-tolerance XYZ-positioning will be integral with all sample chambers.
- J. **Additional user support:** The LERIX-helper package (from Seidler’s group at UW) is now in beta-testing at the Advanced Photon Source. LERIX-helper is a GUI-driven package for calibration and data processing (*i.e.*, re-gridding and statistically-optimal re-binning) for multi-analyzer instruments working in the inverse-scanning mode. This package will be scaled-up and slightly modified for use with LERIX-2, and will then transfer easily to use with XELS. This package allows users to view final energy loss spectra, averaged over selected q , immediately upon completion of energy scanning. Rough, interim spectra (as a function of incident photon energy) will also be computed in real-time during data collection using standard beamline support software.

XELS: Measurement Times for O K-edge Extended XRS Studies

sample	1-analyzer rate (counts/sec) $I_0 = 1 \times 10^{14}/\text{sec}$	estimated bground/step	1-analyzer int. time for 0.3% statistics (min)	30 analyzer total time for study (hrs)
TiO ₂ (bare)	2000	1.7	5.5	0.5
LiTiO ₂ (in situ)	2000	4	18.8	1.6
LiCoO ₂ (in situ)	640	4	58.6	4.9
CO ₂ (100 atm)	4000	2	3.4	0.3
UO ₂	320	5	168.8	14.1

Table 3: Estimated measurement times for several different O K extended XELS studies, all at $q = 8 \text{ \AA}^{-1}$ with 1 eV incident bandwidth. The calculations are based on a combination of theoretical values for the O 1s edge step in the dynamic structure factor, 1×10^{14} ph/sec incident flux at ~10 keV, detection bandwidth and integral reflectivity appropriate for stress-relaxed Si 660 analyzers, and calculated penetration lengths and/or known experimental constraints on scattering lengths. The column “1-analyzer rate ...” gives the anticipated O 1s edge-step height in counts per second as measured by a single Si 660 analyzer. The column “1-analyzer int. time....” gives the needed integration time in minutes for a single analyzer to achieve Poisson statistics, including the dominant Compton background from all sample constituents, at the level of 0.3% of the O K edge-step. In other words, the resulting spectra are targeted to have 300:1 signal to noise after subtraction of the Compton tail. We assume that ~200 individual energies must be measured for a completed study of the extended XELS from an O K-edge. The longer measurement time for in situ battery studies are due to the added Compton scattering signal from the polymer electrolyte matrix which holds the TMO particles. The in situ battery studies would have to be supplemented with measurement of the ~20% O K-edge signal of the polymer electrolyte and (ideally) matching ex situ studies for additional validation. The estimated count rates, above, are also in reasonable agreement with prior experience at the APS LERIX-1 instrument, after scaling for differences in beam and analyzer characteristics. Near-edge studies, also at 1 eV incident bandwidth, would typically require only ~70 energy steps and also would often place much less stringent requirement on signal to noise, so that such measurements would be ~1 order of magnitude faster.

- 1 B. Dickinson, et al. *Rev. Sci. Instrum.* **79**, 123112 (2008)
- 2 XAS-XES beamline ID26 at ESRF: <http://www.esrf.eu/UsersAndScience/Experiments/DynExtrCond/ID26/>
- 3 Kane et al. (2008) *Anal. Chem.* **80**, 9534
- 4 Solomon et al. (2007) PNAS **104**, 4931
- 5 S. Jeffra and M. Francois, *Nature Geoscience*, **2** (2009)
- 6 B. Mishra, J. Fein, N. Yee, T. Beveridge, S. Myneni, *Nature Geoscience*, (In review)
- 7 J.C. Woicik, et al. , *Appl. Phys. Lett.* **73**, 1269 (1998).
- 8 M.O. Krause and J.H. Oliver, *J. Phys. Chem. Ref. Data* **8**, 329 (1976).
- 9 K. Hämmäläinen, et al. *Phys. Rev. B* **46** 14274 (1992).
- 10 E.Jensen, et al., *Phys. Rev. Lett.* **62**, 71 (1989)
- 11 K. Hämmäläinen, et al., *Phys. Rev. Lett.* **67**, 2850 (1991).
- 12 M. Balasubramanian and G. Seidler, private communication
- 13 A 1 micron change in gap on the NSLS-II U20 corresponds to a 5 volt change in peak energy at 17 keV. At that energy, a 0.5 eV step is commonly used in a XANES scan. A repeatable 100 nanometer step in gap height is unrealistic.
- 14 G. Bunker, *Introduction to XAFS: A Practical Guide to X-ray Absorption Fine Structure Spectroscopy*, (2010) Cambridge University Press, [ISBN 978-0521767750](https://doi.org/10.1017/9780521767750)
- 15 M. Rowan, J.W. Peck and T. Rabedeau, *Nucl. Instrum. and Methods, A* **467**, p. 400 (2001)
- 16 J. Woicik et al. *J. Synchrotron Rad.* **17** (2010) 409-413 [doi:10.1107/S0909049510009064](https://doi.org/10.1107/S0909049510009064)
- 17 P. Glatzel, et al. *Catalysis Today* **145** (2009) 294–299 . [doi:10.1016/j.cattod.2008.10.049](https://doi.org/10.1016/j.cattod.2008.10.049)
- 18 *Source Power Load Consideration*, Accel presentation to NSLS-II, August 2007
- 19 NSLS User Administration Office, private communication
- 20 P. Glatzel and U. Bergmann, *Coordination Chemistry Reviews* **249** (2005) 65–95
- 21 J. Yano et al, *J. Am. Chem. Soc.* **127** (2005) pp 14974–14975
- 22 T.T Fister et al., *Rev. Sci. Instrum.* **77**, 063901 (2006), [doi: 10.1063/1.2204581](https://doi.org/10.1063/1.2204581)
- 23 Unpublished work by the spokesperson and collaborators from University of Sheffield.
- 24 S. Huotari et al, *Rev. Sci. Instrum.* **77** 053102 (2006)
- 25 P. Glatzel, private communication
- 26 P. Glatzel, et al. *J. Chem Soc. Am.* **126** (2004) 9946
- 27 R. Vereni, et al, *J. Synchrotron Rad.* **16** 469 (2009); [doi:10.1107/S090904950901886X](https://doi.org/10.1107/S090904950901886X)
- 28 S. Huotari, et al, *J. Synchrotron Rad.* **12** 467 (2005); [doi:10.1107/S0909049505010630](https://doi.org/10.1107/S0909049505010630)

Name: Bruce Ravel (ISS Spokesperson)

Education/Training:

Institution and Location	Degree	Year	Field of Study
University of Washington	Ph.D	1997	Physics
Wesleyan University	B.A.	1989	Physics (<i>magna cum laude</i>)

Research and Professional Experience:

<u>National Institute of Standards and Technology</u>	Scientist, Synchrotron Measurement Group	Nov. 2007-present
	National Research Council Postdoctoral Fellow	1997-1999
<u>Argonne National Laboratory</u>	Physicist, Biology Division	2005-2007
<u>Naval Research Laboratory</u>	Physicist, Chemistry Division	2001-2005
<u>Centre Nationale de la Recherche Scientifique</u>	Visiting scientist	2000-2001

Professional Activities:

- Beamline experience
 - Local contact, beamline X23A2 2007-present
 - Staff member, APS Sector 10, 2005-2007
- Committees
 - Executive committee member, International X-ray Absorption Society, 2005-present
 - Chair, NSLS User Executive Committee, 2009-2010
- XAS software and education
 - Organizer/instructor XAS Schools: NSLS (2003-2005, 2008, 2009), APS (2006-2009), SLS (2007,2009), Thai Synchrotron (2009,2010), Univ. Alberta (2005), Polish Academy of Science (2006), Univ. Ghent (2010)
 - Co-author of the IFEFFIT package, a widely used package for XAS data analysis, 2001-present
 - Contributing author of FEFF8, a widely used XAS theory program
- Review Panels
 - Proposal Review Panel, National Synchrotron Light Source, 2007-present
 - Proposal Review Panel, Advanced Photon Source, 2006-present
 - Proposal Review Panel, Canadian Light Source, 2006-present

Selected Publications:

1. *ATHENA, ARTEMIS, HEPHAESTUS: data analysis for X-ray absorption spectroscopy using IFEFFIT*, B. Ravel and M. Newville, *J. Synchrotron Rad.* **12**, pp. 537-541 (2005), [doi:10.1107/S0909049505012719](https://doi.org/10.1107/S0909049505012719)
At 706 citations, this is the most frequently cited article from The Journal of Synchrotron Radiation.
2. *Real Space Multiple Scattering Calculation and Interpretation of X-Ray Absorption Near Edge Structure*, A.L. Ankudinov, B. Ravel, J.J. Rehr, S. Conradson, *Phys. Rev* **B58**:12, 7565, (1998), [doi:10.1103/PhysRevB.58.7565](https://doi.org/10.1103/PhysRevB.58.7565)
3. *Simultaneous XAFS measurements of multiple samples*, B. Ravel, C. Scorzato, D.P. Siddons, S.D. Kelly, S.R Bare, *J. Synchrotron Radiat.*, **17** (2010) 380-385, [doi:10.1107/S0909049510006230](https://doi.org/10.1107/S0909049510006230)
4. *Performance of a four-element Si drift detector for X-ray absorption fine-structure spectroscopy: resolution, maximum count rate, and dead-time correction with incorporation into the ATHENA data analysis software*, J.C. Woicik, B. Ravel, D.A. Fischer, W.J. Newburgh, *J. Synchrotron Radiat.*, **17** (2010) 409-413, [doi:10.1107/S0909049510009064](https://doi.org/10.1107/S0909049510009064)
5. *The structure of ion beam amorphised zirconolite studied by grazing angle X-ray absorption spectroscopy*, D.P. Reid, M.C. Stennett, B. Ravel, J.C. Woicik, N. Peng, E.R. Maddrell and N.C. Hyatt, *Nuclear Instruments and Methods in Physics Research B* **268**:11-12, (2010) 1847-1852; [doi:10.1016/j.nimb.2010.02.026](https://doi.org/10.1016/j.nimb.2010.02.026)
6. *Condensed Matter Astrophysics: A Prescription for Determining the Species-specific Composition and Quantity of Interstellar Dust Using X-rays*, J.C. Lee, J. Xiang, B. Ravel, J. Kortright K. Flanagan, *The Astrophysical Journal* **702**:2 (2009) 970; [doi: 10.1088/0004-637X/702/2/970](https://doi.org/10.1088/0004-637X/702/2/970)
7. *Protein Oxidation Implicated as the Primary Determinant of Bacterial Radioresistance* M. J. Daly, E. K. Gaidamakova, V. Y. Matrosova, A. Vasilenko, M. Zhai, R. D. Leapman, B. Lai, B. Ravel, S.-M. W. Li, K. M. Kemner, J. K. Fredrickson *PLOS Biology* **5**:4, (2007), [doi:10.1371/journal.pbio.0050092](https://doi.org/10.1371/journal.pbio.0050092)

Anatoly I. Frenkel
Biographical Sketch

Education and Training

Undergraduate, graduate: University of St. Petersburg, Russia, M.S, Physics, 1981-1987

Graduate: Tel-Aviv University, Israel, Ph.D., Physics, 1990-1995

Postdoctoral: University of Washington, Seattle, 1995 – 1996. Postdoctoral advisor: E. A. Stern

Research and Professional Experience

Yeshiva University, Department of Physics. Professor: 2007, Tenure: 2004, Assoc. Professor: 2001

Brookhaven National Lab., NSLS. Visiting Scientist, sabbatical appointment: Jan-May, 2009

U. of Illinois, Urbana-Champaign. Research Scientist at XAFS beamline (X16C), 1996 – 2001

Synergistic activities

- Synchrotron Catalysis Consortium (SCC). Principal Investigator and the Spokesperson.
- Co-organizer, International Operando-IV Congress, Brookhaven National Laboratory, 2012.
- Research interests: In situ x-ray studies of nanomaterials; x-ray studies of reactivity; metal-insulator transitions; polarity of thin films; development of synchrotron instrumentation and data analysis methods.
- Guest editor of two special issues of Synchrotron Radiation News focusing on “Catalysis with Hard X-rays”, published in 2009.
- Organizer and instructor in synchrotron summer schools and short courses in 2001-2009.
- I have been a member of the NSLS Users Executive Committee, NSLS, APS and SSRL Proposal Study Panels, APS AMOC science reviewer, DOE and NSF proposal reviewer.
- Chair of the Division of Natural Sciences and Mathematics at Yeshiva University

Representative publications (total number 155).

- S. Khalid, W. Caliebe, P. Siddons, I. So, B. Clay, T. Lenhard, J. C. Hanson, Q. Wang, A. I. Frenkel, N. Marinkovic, N. Hould, G. Landrot, D. L. Sparks, A. Ganjoo “*QEXAFS instrument with milli-second time scale optimized for in situ applications*” *Rev. Sci. Instrum.* **81**, 015105 (2010).
- A. Yevick, A. I. Frenkel “Effects of surface disorder on EXAFS modeling of metallic clusters” *Phys. Rev. B* **81**, 115451-7 (2010)
- A. Kowal, M. Li, M. Shao, K. Sasaki, M. B. Vukmirovic, J. Zhang, N. S. Marinkovic, P. Liu, A. I. Frenkel, R. R. Adzic “*Ternary Pt/Rh/SnO₂ Electrocatalysts for Oxidizing Ethanol to CO₂*”, *Nature Materials*, **2009**, *8*, 325-330.
- E. Poverenov, I. Efremenko, A. I. Frenkel, Y. Ben-David, L. J. W. Shimon, G. Leituss, J. M. L. Marin, D. Milstein, “A terminal Pt(IV)-oxo complex bearing no stabilizing electron withdrawing ligands and exhibiting diverse reactivity”, *Nature*, **2008**, *255*, 1093-1096.
- Q. Wang, J. C. Hanson, A. I. Frenkel “Solving the structure of reaction intermediates by time-resolved synchrotron x-ray absorption fine structure spectroscopy” *J. Chem. Phys.* **2008**, *129*, 234502
- A. I. Frenkel “Solving the 3D structure of metal nanoparticles”, *Zeitschrift fur Kristallographie*, **2007**, *222*, 605-611. Invited article for the special issue "Structure Studies of Nanocrystals."
- A. I. Frenkel, D. M. Pease, J. Budnick, P. Metcalf, E. A. Stern, P. Shanthakumar, T. Huang ”Strain-induced bond buckling and its role in insulating properties of Cr-doped V₂O₃” *Phys. Rev. Lett.* **2006**, *97*, 195502.
- A. I. Frenkel, A. V. Kolobov, I. K. Robinson, J. O. Cross, Y. Maeda, and C. E. Bouldin, “Direct separation of SRO in intermixed nanocryst. and amorph. phases” *Phys. Rev. Lett.* **2002**, *89*, 285503.

BIOGRAPHICAL SKETCH

NAME		POSITION TITLE	
Jen Bohon		Instructor	
EDUCATION/TRAINING			
INSTITUTION AND LOCATION	DEGREE	YEARS	FIELD OF STUDY
Johns Hopkins University, Baltimore, MD	B.A.	1992-1996	Biology
Stony Brook University, Stony Brook, NY	Ph.D.	1996-2004	Physiology & Biophysics
Brookhaven National Laboratory, Upton, NY	Postdoctoral	2004-2005	Biophysics
Case Western Reserve U., Cleveland, OH	Postdoctoral	2005-2009	Biophysics

A. Professional Positions and Honors

Positions and Employment

1996-2004	Research Assistant, Stony Brook University, Stony Brook, NY
2004-2005	Postdoctoral Research Associate, Brookhaven National Laboratory, Upton, NY
2005-2009	Postdoctoral Fellow and Beamline Scientist, Case Western Reserve University, Cleveland, OH
2009-2010	Senior Research Associate and Beamline Scientist, CWRU, Cleveland, OH
2010-	Instructor and Beamline Scientist, CWRU, Cleveland, OH

Honors

2007-2008	Ruth L. Kirschstein National Service Award, Cell Physiology
2008-2009	Ruth L. Kirschstein National Service Award, Heart and Lung Physiology
2009-	General Member, NSLS User Executive Committee, Elected May 2009

B. Selected Peer Reviewed Publications

1. Bohon, J. and de los Santos, C.R. (2003) Structural effect of the anti-cancer agent 6-thioguanine on duplex DNA. *Nucleic Acids Research*, **31**, 1331-1338.
2. Bohon, J. and de los Santos, C.R. (2005) Effect of 6-thioguanine on the stability of duplex DNA. *Nucleic Acids Research*, **33**, 2880-2886.
3. Sullivan MR, Rekhi S, Bohon J, Gupta S, Abel D, Toomey J, Chance MR (2008) Installation and testing of a focusing mirror at beamline X28C for high flux x-ray radiolysis of biological macromolecules. *Review of scientific instruments*, **79(2 Pt 1)**, 025101.
4. Bohon, J., Jennings, L.D., Phillips, C.M., Licht, S., Chance, M.R. (2008) Synchrotron Protein Footprinting Supports Substrate Translocation by ClpA via ATP-Induced Movements of the D2 Loop. *Structure*, **16**, 1157-1165.
5. Jennings, L.D., Bohon, J., Chance, M.R., Licht, S. (2008) The ClpP N-terminus Coordinates Substrate Access with Protease Active Site Reactivity. *Biochemistry* **47**, 11031-11040.
6. Smedley, J., Bohon, J., Wu, Q., Rao, T. (2009) Laser patterning of diamond. Part I. Characterization of surface morphology, *Journal of Applied Physics* **105**, 123107.
7. Smedley, J., Jaye, C., Bohon, J., Rao, T., Fischer, D. (2009) Laser patterning of diamond. Part II. Surface nondiamond carbon formation and its removal, *Journal of Applied Physics* **105**, 123108.
8. Bohon, J., Smedley, J., Muller, E., Keister, J. W., Development of Diamond-Based X-ray Detection for High Flux Beamline Diagnostics, in *Diamond Electronics and Bioelectronics — Fundamentals to Applications III*, edited by P. Bergonzo, J.E. Butler, R.B. Jackman, K.P. Loh, M. Nesladek (Mater. Res. Soc. Symp. Proc. Volume 1203, Warrendale, PA, 2010), 1203-J19-03.
9. Smedley, J., Keister, J. W., Muller, E., Jordan-Sweet, J., Bohon, J., Distel, J., Dong, B. Diamond Photodiodes for X-ray Applications, in *Diamond Electronics and Bioelectronics — Fundamentals to Applications III*, edited by P. Bergonzo, J.E. Butler, R.B. Jackman, K.P. Loh, M. Nesladek (Mater. Res. Soc. Symp. Proc. Volume 1203, Warrendale, PA, 2010), 1203-J17-21.
10. Shi, W., Bohon, J., Han, D., Habte, H., Qin, Y., Cho, M., Chance, M. R. (2010) Structural Characterization of HIV GP41 with the Membrane Proximal External Region, *J. Biol. Chem.*, *in press*.
11. Bohon, J. Muller, E., Smedley, J. (2010) Development of Diamond-Based X-ray Detection for High Flux Beamline Diagnostics, *J Synchrotron Rad.*, submitted.

Name: Joseph C. Woicik

Education/Training:

Institution and Location	Degree	Year	Field of Study
Stanford University, Stanford CA	Ph.D. and M.S.	1989	Applied Physics
Cornell University, Ithaca NY	B.S.	1983	Applied Physics

Research and Professional Experience:

National Institute of Standards and Technology

Senior Physicist	1999-present
Physicist	1991-1999
National Research Council Post Doctoral Fellow	1989-1991

Professional Activities:

Spokesperson, beamline X2A2 National Synchrotron Light Source
Local contact, beamline X24A National Synchrotron Light Source
Staff member, Advanced Photon Source Sector 33, 2002-2004
Chair, International Workshop for New Opportunities in Hard X-ray Photoelectron Spectroscopy: HAXPES 2009, Brookhaven National Laboratory, 5/20/09 – 5/22/09
Chair, Advanced Photon Source Spectroscopy Review Panel, 2003-2005
Member Advanced Photon Source Beamline Review Panel, 2006
Member Department of Energy Instrumentation Review Panel, 2007

Recent Awards:

Department of Commerce Bronze Metal 1998

Selected Publications:

1. Performance of a 4-element Si drift detector for x-ray absorption fine-structure spectroscopy: Resolution, maximum count rate, dead-time correction, and incorporation into the Athena data analysis software, J.C. Woicik, B. Ravel, D.A. Fischer, and W.J. Newburgh, *J. Synch. Rad.* **17**, 409 (2010).
- 2*. Oxygen vacancies in N doped anatase TiO₂: Experiment and first-principles calculations, A.K. Rumaiz, J.C. Woicik, E. Cockayne, H.Y. Lin, G.H. Jaffari, and S.I. Shah, *Appl. Phys. Lett.* **95**, 262111 (2009).
- 3**. A ferroelectric oxide made directly on silicon, M.P. Warusawithana, C. Cen, C.R. Slesman, J.C. Woicik, Y. Li, L.F. Kourkoutis, J.A. Klug, H. Li, P. Ryan, L.-P. Wang, M. Bedzyk, D.A. Muller, L.-Q. Chen, J. Levy, and D.G. Schlom, *Science* **324**, 367 (2009).
- 4*. Phase identification of self-forming Cu-Mn based diffusion barriers on p-SiOC:H and SiO₂ dielectrics using x-ray absorption fine structure, J.M. Ablett, J.C. Woicik, Zs. Tokei, S. List, and E. Dimasi, *Appl. Phys. Lett.* **94**, 042112 (2009).
5. Strain-induced change in local structure and its effect on the ferromagnetic properties of La_{0.5}Sr_{0.5}CoO₃ thin films, C.K. Xie, J.I. Budnick, W.A. Hines, B.O. Wells, and J.C. Woicik, *Appl. Phys. Lett.* **93**, 182507 (2008).
6. Ferroelectric distortion in SrTiO₃ thin films on Si(001) by x-ray absorption fine structure spectroscopy: Experiment and first-principles calculations, J.C. Woicik, E.L. Shirley, C.S. Hellberg, K.E. Andersen, S. Sambasivan, D.A. Fischer, B.D. Chapman, E.A. Stern, P. Ryan, D.L. Ederer, and H. Li, *Phys. Rev. B* **75**, *Rapid Communications*, 140103 (2007).
7. Site-specific valence x-ray photoelectron spectroscopy, J.C. Woicik, *Synchrotron Radiation News* **17**, 48 (2004).
- 8*. Hybridization and bond-orbital components in site-specific x-ray photoelectron spectra of rutile TiO₂, J.C. Woicik, E.J. Nelson, L. Kronik, M. Jain, J.R. Chelikowsky, D. Heskett, L.E. Berman, and G.S. Herman, *Phys. Rev. Lett.* **89**, 077401 (2002).
9. Direct measurement of valence-charge asymmetry by x-ray standing waves, J.C. Woicik, E.J. Nelson, and P. Pianetta, *Phys. Rev. Lett.* **84**, 773 (2000).
- 10*. Bond-length distortions in strained-semiconductor alloys, J.C. Woicik, J.G. Pellegrino, B. Steiner, K.E. Miyano, S.G. Bompadre, L.B. Sorensen, T.-L. Lee, and S. Khalid, *Phys. Rev. Lett.* **79**, 5026 (1997).
11. Diffraction anomalous fine structure: A new x-ray structural technique, H. Stragier, J.O. Cross, J.J. Rehr, Larry B. Sorensen, C.E. Bouldin, and J.C. Woicik, *Phys. Rev. Lett.* **23**, 3064 (1992).
12. Studies of Si - Ge interfaces with Surface EXAFS and photoemission, J.C. Woicik and P. Pianetta, in Synchrotron Radiation Research: Advances in Surface and Interface Science: Issues and Technology, Ed. R.Z. Bachrach, 1992 Plenum Press, New York.

* NSLS/BNL Highlight

** APS/ANL Highlight

NAME: Lonny E. Berman		POSITION TITLE: Physicist	
EDUCATION INSTITUTION AND LOCATION	DEGREE	YEAR	FIELD OF STUDY
The College of Arts and Sciences, Cornell University	A.B. (Honor)	1981	Physics
The Graduate School, Cornell University	M.S.	1983	Applied Physics and Materials Science
The Graduate School, Cornell University	Ph.D.	1988	Applied Physics and Materials Science

Post-Graduate Experience:

1987 - 1989 Assistant Scientist, National Synchrotron Light Source (NSLS), Brookhaven National Laboratory
1989 - 1991 Associate Scientist, NSLS, Brookhaven National Laboratory
1991 - Present Scientist (Physicist) (Tenure Appt. April 1994), NSLS, Brookhaven National Laboratory
2007 - Present Head, Beamline R&D Section, NSLS, Brookhaven National Laboratory

Award:

2000 BSA Science & Technology Award Co-Recipient, Brookhaven National Laboratory

Relevant Panels:

1996 - 1997; 1999 - 0 External Review Board, Industrial Macromolecular Crystallographic Association, Argonne Nat Lab
1997 - 99; 2001 - 2 United States National Committee for Crystallography, National Research Council
1998 - 1999 Technical Advisory Committee, Structural Biology Center Principal Users Group, Argonne Nat Lab
1998 - 2002 Scientific Advisory Board, Southeast Regional Collaborative Access Team, Argonne National Lab
1999 - Present Synchrotron Advisory Board, National Institute of General Medical Sciences, National Inst of Health

Editorships:

2002 - Present Co-Editor, Journal of Synchrotron Radiation, published by the Int Union of Crystallog, Chester, UK

Selected Recent Publications:

1. C.-Y. Kim, M.J. Bedzyk, E.J. Nelson, J.C. Woicik, and L.E. Berman, "Site-Specific Valence-Band Photoemission Study of α -Fe₂O₃", Phys. Rev. B 66, 085115 (2002).
2. J.C. Woicik, E.J. Nelson, L. Kronik, M. Jain, J.R. Chelikowsky, D. Heskett, L.E. Berman, and G.S. Herman, "Hybridization and Bond-Orbital Components in Site-Specific X-Ray Photoelectron Spectra of Rutile TiO₂", Phys. Rev. Lett. 89, 077401 (2002).
3. L.E. Berman, D.P. Siddons, P.A. Montanez, A. Lenhard, and Z. Yin, "A Cryogenically Cooled Channel-Cut Crystal Monochromator Using a Helium Refrigerator and Heat Exchanger", Rev. Sci. Instrum. 73, 1481-1484 (2002).
4. L.E. Berman, Q. Shen, K.D. Finkelstein, P. Doing, Z. Yin, and G. Pan, "Characterization of a Diamond Crystal X-Ray Phase Retarder", Rev. Sci. Instrum. 73, 1502-1504 (2002).
5. J.M. Ablett, L.E. Berman, C.-C. Kao, G. Rakowsky, and D. Lynch, "Small-Gap Insertion Device Development at the National Synchrotron Light Source -- Performance of the New X13 Mini-Gap Undulator", J. Synchrotron Radiation 11, 129-131 (2004).
6. W. Shi, H. Robinson, M. Sullivan, D. Abel, J. Toomey, L.E. Berman, D. Lynch, G. Rosenbaum, G. Rakowsky, L. Rock, W. Nolan, G. Shea-McCarthy, D. Schneider, E. Johnson, R.M. Sweet, and M.R. Chance, "Beamline X29: A Novel Undulator Source for X-Ray Crystallography", J. Synchrotron Rad. 13, 365-372 (2006).
7. R.F. Fischetti, D.W. Yoder, S. Xu, S. Stepanov, O. Makarov, R. Benn, S. Corcoran, W. Diete, M. Schwoerer-Boehing, R. Signorato, L. Schroeder, L.E. Berman, P.J. Viccaro, and J.L. Smith, "Optical Performance of the GM/CA-CAT Canted Undulator Beamlines for Protein Crystallography", Proceedings of the Ninth International Conference on Synchrotron Radiation Instrumentation, AIP Conf. Proc. 879, 754-757 (2006).
8. T. Tanabe, J.M. Ablett, L.E. Berman, D.A. Harder, S. Hulbert, M. Lehecka, G. Rakowsky, J. Skaritka, A. Deyhim, E. Johnson, J. Kulesza, and D. Waterman, "X25 Cryo-Ready In-Vacuum Undulator at the NSLS", Proceedings of the Ninth International Conference on Synchrotron Radiation Instrumentation, AIP Conf. Proc. 879, 283-286 (2006).
9. J.M. Ablett and L.E. Berman, "Spectral Measurements and Synchrotron Radiation Calculation Comparisons of the New X25 Mini-Gap Undulator", Proceedings of the Fourteenth National Conference on Synchrotron Radiation Instrumentation, Nucl. Instrum. Methods Phys. Res., Sect. A 582, 37-39 (2007).
10. T. Shaftan, S. Hulbert, and L. Berman, "Comparison of calculated brightness and flux of radiation from a long-period wiggler and a short-period undulator", J. Synch. Rad. 15, 335-340 (2008).
11. E.M. Dufresne, S.B. Dierker, Z. Yin, and L.E. Berman, "Development of New Apertures for Coherent X-ray Experiments", J. Synch. Rad. 16, 358-367 (2009).
12. J. Dvorak, L.E. Berman, S.L. Hulbert, D.P. Siddons, and K. Wallwork, "Simple Tools for Characterization of Synchrotron Beam Flux, Energy Resolution, and Stability", Proceedings of the Tenth International Conference on Synchrotron Radiation Instrumentation, AIP Conf. Proc. 1234, 639-642 (2009).
13. O. Chubar, J. Bengtsson, L.E. Berman, A. Broadbent, Y.Q. Cai, S. Hulbert, Q. Shen, and T. Tanabe, "Parametric Optimization of Undulators for NSLS-II Project Beamlines", Proceedings of the Tenth International Conference on Synchrotron Radiation Instrumentation, AIP Conf. Proc. 1234, 37-40 (2009).

Paul Northrup

Department of Geosciences, Stony Brook University

Education:

Dowling College	Biology	B.A., 1989
Stony Brook University	Earth and Space Sciences	M.S., 1992
Stony Brook University	Geology	Ph.D., 1996
Bell Laboratories	Post-Doctoral Associate	1996-1998

Appointments:

2009-present	Lecturer and Research Scientist, Department of Geosciences, Stony Brook University
2004-2009	Assistant, Associate Environmental Scientist, Environmental Sciences Department, BNL
2003-2004	Research Scientist, Department of Geosciences, Stony Brook University
1998-2003	Physicist, Member of Technical Staff, Bell Laboratories, Lucent Technologies

NSLS:

2003-present	Spokesperson and Program Director, Beamline X15B
1996-present	Beamline Scientist, Participating Research Team (PRT), X15B
2004-2009	Contributing User Group Beamline Scientist, X27A Microprobe
2004-2009	PRT member, X11A and X11B EXAFS beamlines
2005-2008	Scientist, Center for Environmental Molecular Science, an NSF/DOE Center at BNL and Stony Brook

NSLS-II Project:

2009-present	Beamline Development Scientist (25%), NSLS-II Submicron Resolution X-ray (SRX) Beamline
2008-2009:	Group Leader (interim), SRX Beamline
2008-present	Beamline Advisory Team member, SRX Beamline
2007-2008	Group Leader, NSLS-II Project Beamline for XAS

Selected Relevant Publications:

- P. Northrup, "X-ray Absorption Spectroscopy Beamline", Part 2, Chapter 5, in *NSLS-II Preliminary Design Report (PDR)*, NSLS-II, 2008.
- P. Northrup and R. Reeder, "Evidence for the importance of growth-surface structure to trace element incorporation in topaz" *Am. Min.*, 79, 1994.
- F. Einsiedl, T. Schäfer, and P. Northrup, "Combined sulfur K-edge XANES spectroscopy and stable isotope analyses of fulvic acids and groundwater sulfate identify sulfur cycling in a karstic catchment area" *Chemical Geology* 238, 268-276, 2007.
- P. Bingham, A. Connelly, R. Hand, N. Hyatt, P. Northrup, "Incorporation and Speciation of Sulphur in Glasses for Waste Immobilization" *Glass Technol.*, 50(3), 135-138, 2009.
- P. Northrup, A. Lanzirrotti, A. Celestian, "Growth of Environmental Science at the NSLS" *Synch. Rad. News*, 20:3, 2007.
- P. Voyles, P. Citrin, D. Chadi, D. Muller, J. Grazul, P. Northrup, H.-J. Gossmann, "Evidence for a New Class of Defects in Highly n-doped Si: Donor-pair-vacancy-interstitials" *Phys. Rev. Lett.*, 91, 125505, 2003.
- P. Citrin, P. Northrup, R. Birkhahn, A. Steckl, "Local Structure and Bonding of Er in GaN: A Contrast with Er in Si" *Appl. Phys. Lett.*, 76: 2865, 1999.

Synergistic activities:

- Beamline design:** a) current X15B Helium-atmosphere endstation, design, construction and commissioning, b) NSLS-II beamline for bulk/microbeam XAS, full preliminary design, c) NSLS-II SRX Beamline, collaborator on initial BAT design, adaptation to NSLS-II Project constraints, ongoing design effort.
- Beamline management and program development:** X15B.
- User community:** NSLS User Executive Committee representative for imaging. Workshops, short courses and seminars.
- Facility strategic planning:** Participation in NSLS/NSLS-II scientific and facility strategic planning workshops, and development of white papers.

Trevor Anthony Tyson's Short Curriculum Vitae

Department of Physics
New Jersey Institute of Technology
Newark, New Jersey 07102-1982

Tel. #: (973) 642-4681
FAX #: (973) 596-5794
E-mail: tyson@adm.njit.edu

Professional Preparation

Professor (physics)	New Jersey Institute of Technology	2003-
Associate Professor (physics)	New Jersey Institute of Technology	2000-2003
Member of Graduate Faculty (physics)	Rutgers Univ., Newark Campus	1996-
Assistant Professor (physics)	New Jersey Institute of Technology	1996-2000
Postdoctoral Position	Los Alamos National Laboratory	1994
Postdoctoral Position - Atomic Physics and Spectroscopy		1991
	Stanford University School of Humanities and Sciences Postdoc. Fellow	
	INFN Frascati Italy - Stanford University	
Ph. D. (Applied Physics)		Stanford University 1991
B. S., Honors (Physics with Mathematics Minor)		Andrews University 1983

Related Publications

P. Gao, H. Chen, T. A. Tyson, Z. Liu, and S.-W. Cheong, "Infrared and x-ray absorption measurements of anomalous phonon effects in orthorhombic LuMnO₃: Evidence for an electronically driven ferroelectric state", submitted to Phys. Rev. Lett.

S. Sumit and T. A. Tyson, "New Insights in Electronic Structure and Antiaromatic Instabilities of Boron Nanoribbons", Physical Review Letters, in press.

V. V. Poltavets, K. A. Lokshin, H. Nevidomskyy, M. Croft, T. A. Tyson, J. Hadermann, G. Van Tendeloo, T. Egami, G. Kotliar, N. ApRoberts-Warren, A. P. Dioguardi, N. J. Curro, and M. Greenblatt, "Bulk Magnetic Order in a Two-Dimensional Ni_{1-x}Ni_{2x}(d₉=d₈) Nickelate, Isoelectronic with Superconducting Cuprates", Physical Review Letters, **104**, 206403 (2010).

T. A. Tyson, Z. Chen, Q. Jie, Q. Li and J. J. Tu, "Local Spin-Coupled Distortions in Hexagonal Multiferroic HoMnO₃", Phys. Rev. B **81**, 054101 (2010).

T. A. Tyson, Z. Chen, Q. Jie, Q. Li, and J. J. Tu, "Local structure of thermoelectric Ca₃Co₄O₉", Phys. Rev. B: Condens. Matter Mater. Phys. **79**, 024109/1 (2009).

Q. Qian, T. A. Tyson, M. Deleon, C. C. Kao, J. Bai, and A. I. Frenkel, "Influence of strain on the atomic and electronic structure of manganite films", Journal of Physics and Chemistry of Solids **68**, 458 (2007).

Q. Qian, T. A. Tyson, C. Dubourdieu, A. Bossak, J. P. Sénateur, M. Deleon, J. Bai, and G. Bonfait, "Structural, Magnetic and Transport Studies of La_{0.8}MnO₃ Films", J. Appl. Phys. **92**, 4518 (2002).

Q. Qian, T. A. Tyson, C. Dubourdieu, A. Bossak, J. P. Sénateur, M. Deleon, J. Bai, and G. Bonfait, "[Structural studies of annealed ultrathin La_{0.8}MnO₃ films](#)", Appl. Phys. Lett. **80**, 2663 (2002).

Funding (Active)

[1] T. A. Tyson, "Understanding the Spin-Lattice Coupling in Multiferroic Oxides" DOE-BES (\$640,000, 8/2007 to 7/2011)

[2] T. A. Tyson (NJIT), P. Siddons (BNL), J. Bai (UT), Gianluigi De Geronimo, (BNL), C.-C. Kao (BNL) "Development of a Silicon Detector for Synchrotron Based X-Ray Spectroscopy, X-Ray Holography and Materials Education", NSF MRI (\$550,000, 8/2007 to 7/2010)

[3] T. A. Tyson, T. Zhou, M. Xanthos, Z. Iqbal and N. M. Ravindra, "MRI: Acquisition of a Properties Measurement System for Education and Research in Energy Related Materials", NSF MRI (\$300,000, 9/2009 to 9/2010)

Ph. D Thesis Advisors: K. O. Hodgson (Stanford University, principal advisor)
S. Doniach (Stanford University)

Name: Bruce A. Bunker

Education/Training:

Institution and Location	Degree	Year	Field of Study
University of Washington	Ph.D	1974	Physics
University of Washington	B.A.	1980	Physics

Research and Professional Experience:

University of Notre Dame

Department Chair, Department of Physics	Aug. 1998 – Aug. 2003.
Professor, Department of Physics	Aug. 1994 - present.
Associate Professor, Department of Physics	Aug. 1987 – Aug. 1994.
Assistant Professor, Department of Physics	Sep. 1983 – Aug. 1987.

Professional Activities:

- Director, *Materials Research Collaborative Access Team*, Advanced Photon Source, Argonne National Laboratory.
- Vice Chair and Chair Elect, *Executive Committee, International X-ray Absorption Society*
- Panel Chair, National Science Foundation Review Panel, MIT CUBIX Science and Technology Center, Oct. 11-13, 2009.
- Member, *Partner User Council*, Advanced Photon Source
- Member, General User Program Advisory Committee, Advanced Photon Source.
- Member, Canadian Light Source *Peer Review Committee*, 2006-2008.
- Member, National Science Foundation Review Panel, *Cornell High-Energy Synchrotron Source*, October 15-16 2007, and April 27-29 2009.
- Co-Organizer, XAFS X, The 10th International Conference on X-ray Absorption Fine Structure (XAFS X) (Chicago, Illinois, USA, August 10-14, 1998).

Selected Publications:

1. Mishra, B., Boyanov, M., Bunker, B. A., Kelly, S. D., Kemner K. M., Nerenberg, R., Read-Daily, B. L., Fein, J. B.. “X-ray Absorption Spectroscopy Study of Cd Adsorption Onto Bacterial Consortia”, *Geochimica et Cosmochimica Acta* 73 4311–4325, (2009).
2. Mishra, B., Haack, E. A., Maurice, P. A., and Bunker, B. A. (2009). “Effects of the Microbial Siderophore DFO-B on Pb and Cd Speciation in Aqueous Solution”, *Environ. Sci. Technol.*, 43 (1), pp 94–100, (2009).
3. Vasconcelos, I. F., Haack, E. A., Maurice, P. A., Bunker, B. A., “EXAFS Analysis of Cadmium(II) Adsorption to Kaolinite”, *Chem. Geol.* 249/3-4, 237-250, (2008).
4. Vasconcelos, I. F., Bunker, B. A., and Cygan, R. T., “Molecular Dynamics Modeling of Ion Adsorption to the Basal Surfaces of Kaolinite”, *J. Phys. Chem. C* 111(18) pp 6753 – 6762 (2007) .
5. Mishra, B., Kelly, S. D., Fein, J. B., Boyanov, M., Kemner, K. M. and Bunker, B. A.. “Cd adsorption onto *Bacillus subtilis* bacterial cell walls: Integrating isotherm and EXAFS studies” *Geochimica Et Cosmochimica Acta* 69 A675-a675, (2005)
6. Robel, I. Girishkumar, G., Bunker, B. A., Kamat, P. V., Vinodgopal, K. (2006). “Structural changes and catalytic activity of platinum nanoparticles supported on C60 and carbon nanotube films during the operation of direct methanol fuel cells”, *App. Phys. Lett.* 88, 073113-1-3.
7. Lahiri, D., Subramania, V., Bunker, B. A., and Kamat, P. V. (2006). “Probing Photochemical Transformations at TiO2/Pt and TiO2/Ir interfaces using X-ray Absorption Spectroscopy”, *J. Chem. Phys.* 124 (20), 204720-1-204720-7.
8. Robel, I., Bunker, B. A., Kamat, P. V. and Kuno, M. (2006). "Exciton recombination dynamics in CdSe nanowires: Bimolecular to three-carrier Auger kinetics" *Nano Letters* 6(7): 1344-1349 (2006).
9. Lahiri, D., Bunker, B. A., Mishra, B., Zhang, Z., Meisel, D., Doudna, C. M., Bertino, M. F., Blum, F. D., Tokuhira, A. T., S. Chattopadhyay, Shibata, T., Terry, J. (2005). “Bimetallic Pt–Ag and Pd–Ag nanoparticles”, *J. Applied Phys.*, 97, 094304.
10. Robel, I., Bunker, B. A., and Kamat, P. V.. "SWCNT-CdS nanocomposite as light harvesting assembly: Photoinduced charge transfer interactions", *Adv. Mater.*, 17, 2458-2463 (2005).

BIOGRAPHICAL SKETCH

NAME Mark R. Chance		POSITION TITLE Director and Professor		
EDUCATION/TRAINING (Begin with baccalaureate or other initial professional education, such as nursing, and include postdoctoral training.)				
INSTITUTION AND LOCATION		DEGREE	YEAR(s)	FIELD OF STUDY
Wesleyan University, Middletown, CT		B.A.	1980	Biology
MIT, Boston, MA			1980-1984	Biochemistry
University of Pennsylvania, Philadelphia, PA		Ph.D.	1986	Biophysics
AT&T Bell Labs, Murray Hill, NJ		Post-Doc	1986-1988	Biophysics

A. Professional Positions

Positions and Employment

- 1995- Director, Center for Synchrotron Biosciences, NSLS, Brookhaven Labs (BNL)
2005- Director, Case Center for Proteomics and Cleveland Foundation Center for Proteomics
2005- Professor of Physiology & Biophysics, Case Western Reserve Medical School, Cleveland OH
2007- Director, Translational Technologies Core, Cleveland Center for Translational Science

National and International Committees

- 2003- Scientific Advisory Committee, Protein Crystallography Research Resource, BNL, Chair (2007)
2007-2010 Experimental Facilities Advisory Committee, National Synchrotron Light Source-II, BNL
2006-2010 Biophysics Proposal Review Panel, Advanced Light Source, Lawrence Berkeley National Lab.
2009- Editorial Board Member, Cancer Genomics and Proteomics
2009 Reviewer, Research Grants Council, Hong Kong, China

B. Selected Recent Publications

1. Angel, T., Chance, M.R., and Palczewski, K. Conserved waters mediate structural and functional activation of family A (rhodopsin-like) G protein-coupled receptors, *Proc. Nat. Acad. Sci.*, 106(21):8555-60, 2009. PMID: PMC2688986
2. Angel, T.E., Gupta, S., Jastrzebska, B., Palczewski, K., Chance, M.R. "Structural waters define a functional channel mediating activation of the GPCR, rhodopsin", *Proc. Nat. Acad. Sci.*, 106(34):14367-72, 2009. PMID: PMC2732891
3. Kiser, P., Golczak, M., Lodowski, D., Chance, M.R., Palczewski, K., "Crystal Structure of Native RPE65, the Retinoid Isomerase of the Visual Cycle", *Proc. Nat. Acad. Sci.*, 106(41):17325-30, 2009. PMID: PMC2765077
4. Orban, T., Gupta, S., Palczewski, K., Chance, M.R. "Visualizing Water Molecules in Transmembrane Proteins Using Radiolytic Labeling Methods," *Biochemistry*, 49(5):827-34, 2010. PMID: PMC2819031
5. Orban, T., Bereta, G., Miyagi, M., Wang, B., Chance, M.R., Sousa, M.C., Palczewski, K. "Conformational Changes in Guanylate Cyclase-Activating Protein 1 Induced by Ca²⁺ and N-Terminal Fatty Acid Acylation," *Structure*, 18(1):116-26, 2010. PMID: PMC2822722
6. Gupta, S., Bavro, V.N., D'Mello, R., Tucker, S.J., Venien-Bryan, C., Chance, M.R. "Conformational Changes During the Gating of a Potassium Channel Revealed by Structural Mass Spectrometry," *Structure*, in press, 2010.

C. Research Support

Ongoing Research Support

- P30-EB-009998 (Chance)** 9/09-8/14
NIH
Case Center for Synchrotron Biosciences
- P20-DA-026133 (Chance)** 4/09-3/12
NIH
Case Center for Proteomics in HIV/AIDS and Drug Abuse
- P30-EB009998 (Chance)** 9/09-8/14
NIH
Case Center for Synchrotron Biosciences
- P01-AI-074286 (Cho)** 4/08-3/11
NIH
Development of a Subunit Envelope Vaccine
Mark Chance – co-PI- Project 2-Structural Evaluation of Antigens
- P01-DE-019759 (Weinberg)** 3/09-2/14
NIH
Oral Mucosal Immunity in Vulnerable HIV Infected Populations
- UL1-RR-024989 (Davis)** 9/07-8/12
NIH
Case Western Reserve University/Cleveland Clinic CTSA
Mark Chance - PI of Translational Technology Core

Simon R. Bare
Biographical Sketch

Education and Training

Undergraduate: University of Liverpool, UK, B.Sc. (Hons), 1979

Graduate: University of Liverpool, UK, Ph.D., Chemistry, 1982

Postdoctoral: Cornell University, Ithaca, NY, 1982-1984. Postdoctoral advisor: Wilson Ho

Postdoctoral: Lawrence Berkeley National Laboratory, Berkeley, CA, 1984-1986. Postdoctoral advisor: Gabor A. Somorjai

Research and Professional Experience

UOP LLC, a Honeywell Company, Des Plaines, IL

Senior Principal Scientist, 2003–present, Research & Development Associate 1996-2003

The Dow Chemical Company, Midland, MI

Research Leader, 1993-1996, Project Leader 1989-1993, Senior Research Chemist 1986-1989

Synergistic Activities:

- Synchrotron Catalysis Consortium (SCC). Industrial member
- Member of Basic Energy Sciences Advisory Committee (BESAC)
- Member of BNL Light Sources Directorate Scientific Advisory Committee
- Co-organizer, International Operando-IV Congress, Brookhaven National Laboratory, 2012.
- Chair of DMSE COV, panel lead SUFD COV
- Former member of the NSLS Users Executive Committee (including Chair), NSLS and APS Proposal Study Panels, DOE and NSF proposal reviewer.
- Initiator of inaugural course on EXAFS Data Collection & Analysis, 2003. Co-organized similar course at NSLS and APS. Lectured at course (2003-5, 2007)
- Research interests: Characterization of catalysts, with focus on in situ characterization. Fundamental surface chemistry of catalysts. Synchrotron-radiation based X-ray methods for probing the structure of catalysts. Developing structure-activity relationships in catalysis.

Representative Publications (total number 70+):

- "Characterization of catalysts in reactive atmospheres by X-ray absorption spectroscopy", S.R. Bare and T. Ressler, *Advances in Catalysis*, (2009) **52** 339-465.
- "Structural Characterization of Ni-W hydrocracking catalyst using in situ EXAFS and HRTEM", S.D. Kelly, N. Yang, G.E. Mickelson, N. Greenlay, E. Karapetrova, W. Sinkler, S.R. Bare. *J. Catalysis* (2009) **263** 16-33.
- "Design and operation of a high pressure reaction cell for in situ x-ray absorption spectroscopy", S.R. Bare, N. Yang, S.D. Kelly, G.E. Mickelson, and F.S. Modica, *Catalysis Today* (2007) **126** 18-26
- "Uniform catalytic site in Sn- β zeolite determined using x-ray absorption fine structure", S.R. Bare, S.D. Kelly, W. Sinkler, J.J. Low, F.S. Modica, S. Valencia, A. Corma, L.T. Nemeth, *J. Am. Chem. Soc.* **127** (2005) 12924-12932.
- "Effect of hydrogen adsorption on the X-ray absorption spectra of small Pt clusters", A.L. Ankudinov, J.J. Rehr, J.J. Low, S.R. Bare, *Phys. Rev. Lett.*, **86** (2001) 1642-1645.
- "The kinetic significance of V⁵⁺ in n-butane oxidation catalyzed by vanadium phosphates", G.W. Coulston, S.R. Bare, H.H. Kung, K.E. Birkeland, G. Bethke, R. Harlow, N. Herron, P.L. Lee, *Science*, **275** (1997) 191-193.
- "Simple flow-through reaction cells for in situ transmission and fluorescence X-ray absorption spectroscopy of heterogeneous catalysts", S.R. Bare, G.E. Mickelson, F.S. Modica, A.Z. Ringwelski, and N. Yang, *Rev. Sci. Instrum.*, (2006) **77** 023105/1-023105/6.

Name: Gerald T. Seidler

Education/Training:

Institution and Location	Degree	Year	Field of Study
University of Chicago	Ph.D	1993	Physics
University of Chicago	M.Sc.	1991	Physics
University of Florida	B.Sc.	1988	Physics

Research and Professional Experience:

<u>University of Washington</u>		
Associate Professor, Department of Physics		2002-present
Assistant Professor, Department of Physics		1996-2002
<u>NEC Research Institute, Princeton NJ</u>		
Research Scientist		1993-1996

Professional Activities:

- Applications and spectrometer development for high-throughput nonresonant inelastic x-ray scattering from valence- and core-level initial states. This includes the design and construction of the LERIX spectrometer at the Advanced Photon Source.
- Applications and spectrometer development for high-throughput resonant and nonresonant x-ray emission spectroscopy. This includes the development of the miniXS spectrometers for rapid XES studies, such as at the 20-ID XAS microprobe endstation at the Advanced Photon Source.
- Energy sciences research, involving actinide materials, energy storage systems, and polymeric photovoltaics

Selected Publications:

1. *A Comparative Study of the Valence Electronic Excitations of N₂ by Inelastic X-ray and Electron Scattering*, J.A. Bradley, G.T. Seidler, G. Cooper, M. Vos, A.P. Hitchcock, A.P. Sorini, C. Schlimmer, K.P. Nagle, **submitted**, Phys Rev Lett (2010).
2. *NaReO₄, An Intensity Standard for O K-edge Covalency Studies Using XAS and NRIXS Spectroscopy*, J.A. Bradley, E.R. Batista, K.S. Boland, C.J. Burns, D.L. Clark, S.D. Conradson, S.A. Kozimor, R.L. Martin, G.T. Seidler, D.K. Shuh, T. Tylliszczak, M.P. Wilkerson, L.E. Wolfsberg, Ping Yang, **accepted**, J Amer Chem Soc (2010).
3. *Probing Electronic Correlations in Actinide Materials Using Multipolar Transitions*, J.A. Bradley, S. Sen Gupta, G.T. Seidler, K.T. Moore, M.W. Haverkort, G.A. Sawatzky, S.D. Conradson, D.L. Clark, S.A. Kozimor, and K.S. Boland, Phys Rev **B81:19** 193104 (2010).
4. *Momentum-resolved Resonant and Nonresonant Inelastic X-ray Scattering at the Advanced Photon Source*, T. Gog, G.T. Seidler, D.M. Casa, *et al.*, Synchrotron Radiation News **22:6** 12 (2009).
5. *Intermediate-Range Order in Water Ices: Non-resonant inelastic x-ray scattering measurements and real-space full multiple scattering calculations*, T. T. Fister, K. P. Nagle, F. D. Vila, G. T. Seidler, J. J. Rehr, J. O. Cross, and C. Hamner, Phys Rev **B79** 174117 (2009).
6. *A Short Working Distance Multiple Crystal X-ray Spectrometer*. B. Dickinson, G.T. Seidler, Z.W. Webb, J.A. Bradley, K.P. Nagle, S.M. Heald, R.A. Gordon, and I.M. Chou, Rev Sci Instrum **79**, 123112 (2008).
7. *The local electronic structure of α -Li₃N*, T. T. Fister, G. T. Seidler, E. L. Shirley, F. D. Vila, J. J. Rehr, K. P. Nagle, J. C. Linehan, and J. O. Cross, J Chem Phys **129** 044702 (2008).
8. *An extraction algorithm for core level excitations in non-resonant inelastic x-ray scattering spectra*, H. Sternemann, C. Sternemann, G. T. Seidler, T. T. Fister, and M. Tolan, J Synch Rad **15:2** 162 (2008).
9. *The Local Electronic Structure of Dicarba-closo-dodecarboranes C₂B₁₀H₁₂*, T.T. Fister, F.D. Vila, G.T. Seidler, L. Svec, J.C. Linehan, J.O. Cross, J Amer Chem Soc **130** 925 (2008).
10. *High multipole transitions in NIXS: valence and hybridization in 4f systems*, R.A. Gordon, G.T. Seidler, T.T. Fister, M.W. Haverkort, G.A. Sawatzky, A. Tanaka, and T.K. Sham, EPL **81** 26004 (2008).
11. *Fine Structure and Chemical Shifts in Non-resonant Inelastic x-ray Scattering from Li-intercalated Graphite*, M. Balasubramanian, C.S. Johnson, J.O. Cross, G.T. Seidler, T.T. Fister, E.A. Stern, C. Hamner, and S.O. Mariager, Appl Phys Lett **91** 031904 (2007).
12. *Deconvolving Instrumental and Intrinsic Energy Resolution in Excited- State X-ray Spectroscopies*, T.T. Fister, G.T. Seidler, J.J. Rehr, J.J. Kas, W.T. Elam, J.O. Cross, and K.P. Nagle, Phys Rev **B75** 174106 (2007).
13. *A multielement spectrometer for efficient measurement of the momentum transfer dependence of inelastic x-ray scattering*, T.T. Fister, G.T. Seidler, L. Wharton, *et al.*, Rev Sci Instrum **77** 063901 (2006).

Serena DeBeer

Education/Training:

Institution and Location	Degree	Year	Field of Study
Stanford University	Ph.D.	2002	Inorganic Chemistry
Southwestern University	B.S.	1995	Chemistry (with honors)

Research and Professional Experience:

2009-present	Assistant Professor, Cornell University
2003-2009	Staff Scientist, Stanford Synchrotron Radiation Laboratory
2001-2003	Beam line Scientist, Stanford Synchrotron Radiation Laboratory
1995-2001	Graduate Research Assistant, Department of Chemistry, Stanford University
1996-1999	Advanced Teaching Assistant, Department of Chemistry, Stanford University
1995-1996	Teaching Assistant, Department of Chemistry, Stanford University

Professional Activities:

Co-chair, Structural Molecular Biology Synchrotron Summer School, SSRL (2003-2007).
Lecturer, Berkeley-Stanford Summer School on Synchrotron Radiation, 2006
Lecturer, Advanced Photon Source XAFS School, 2009
Organizer XAS Short Course, SSRL 2007
Co-chair of a STXM workshop for applications in geological, environmental and biological sciences, SSRL, 2007
Co-chair of a workshop on XANES spectroscopy at the SSRL, 2007
Proposal Review Panel, Advanced Photon Source, 2008-2009
Guest editor of a special issue of *Inorganica Chimica Acta*
Lecturer, Synchrotron School, National Synchrotron Radiation Laboratory, Thailand, 2005-2007

Selected Publications:

1. “Probing Valence Orbital Composition with Iron K β X-ray Emission Spectroscopy” N. Lee, T. Petrenko, U. Bergmann, F. Neese, S. DeBeer, *J. Am. Chem. Soc.*, *in press*.
2. “Calibration of Scalar Relativistic Density Functional Theory for the Calculation of Sulfur K-Edge Absorption Spectra” S. DeBeer George, F. Neese, *Inorg. Chem.*, **2010**, *49*, 1849-1853.
3. “Type zero copper proteins”, K. M. Lancaster, S. DeBeer George, K. Yokoyama, J. H. Richards, H. B. Gray, *Nature Chem.*, **2009**, *1*, 711-715.
4. “Polarized X-ray Absorption Spectroscopy of Single-crystal Mn(V) Complexes Relevant to the Oxygen Evolving Complex of Photosystem II” J. Yano, J. Robblee, Y. Pushkar, M. A. Marcus, K. Sauer, J. Bendix, T. J. Collins, E. I. Solomon, S. DeBeer George, and V. Yachandra, *J. Am. Chem. Soc.*, **2007**, *129*, 12989-13000.
5. “Characterization of a Genuine Iron(V) Nitrido Species by Nuclear Resonant Vibrational Spectroscopy Coupled to Density Functional Calculations” S. DeBeer George, T. Petrenko, N. Aliaga-Alcade, E. Bill, B. Mienert, W. Sturhahn, Y. Xiao, K. Wieghardt, F. Neese, *J. Am. Chem. Soc.*, **2007**, *129*, 11053-11060.
6. “An Octahedral Coordination Complex of Iron(VI)” J. F. Berry, E. Bill, E. Bothe, S. DeBeer George, B. Mienert, F. Neese, K. Wieghardt, *Science*, **2006**, *312*, 1937-1941.

Wendy Mao

Education/Training:

Institution and Location	Degree	Year	Field of Study
University of Chicago	Ph.D.	2005	Geophysical Sciences
MIT	B.S.	1998	Materials Science & Engineering

Research and Professional Experience:

Stanford University

Assistant Professor, Joint appointment in Geological and Environmental Sciences & Photon Science, SLAC National Accelerator Laboratory 2007-present

Los Alamos National Laboratory

J. R. Oppenheimer Fellow, Post-Doc 2005-2007

Professional Activities:

- Elected member of COMPRES Facilities Committee
- Elected member of APS Users Organization Steering Committee
- DOE Hydrogen Fuel Initiative Review, Hydrogen Storage Panel Member
- West Coast High Pressure Facilities Review Committee, Advanced Light Source, Lawrence Berkeley National Laboratory
- National School on Neutron and X-ray Scattering, Argonne National Laboratory, Argonne, IL, 2008-present.

Selected Publications:

1. “S. Wang, **W. L. Mao**, A. P. Sorini, C-C. Chen, T. P. Devereaux, Y. Ding, Y. Xiao, P. Chow, N. Hiraoka, H. Ishii, Y. Q. Cai, and C-C. Kao, High pressure evolution of Fe₂O₃ electronic structure revealed by X-ray absorption spectroscopy, *Phys. Rev. Lett.*, submitted.
2. L. Wang, Y. Ding, W. Yang, W. Liu, Z. Cai, J. Kung, J. Shu, R. J. Hemley, **W. L. Mao**, and H.-k. Mao, Nanoprobe measurements of materials at megabar pressures, *Proc. Nat. Acad. Sci.*, doi:10.1073/pnas.1001141107, 2010.
3. Q. Zeng, Y. Ding, **W. L. Mao**, W. Yang, S. V. Sinogeikin, J. Shu, H-k. Mao, and J.Z. Jiang, Origin of pressure-induced polyamorphism in Ce₇₅Al₂₅ metallic glass, *Phys. Rev. Lett.* **104**, 105702, 2010.
4. M. Baldini, G. Aquilanti, H-k. Mao, W. Yang, G. Shen, S. Pascarelli, and **W. L. Mao**, High-pressure EXAFS study of vitreous GeO₂ up to 44 GPa, *Phys. Rev. B* **81**, 024201, 2010.
5. T. Yamanaka, **W. L. Mao**, H-k. Mao, R. J. Hemley, and G. Shen, New structure and spin state of iron-rich (Mg,Fe)SiO₃ post-perovskite, *J. Phys.: Conf. Ser.* **215** 012100, doi: 10.1088/1742-6596/215/1/012099, 2010.
6. Q. Zeng, Y. Ding, **W. L. Mao**, W. Luo, A. Blomqvist, R. Ahuja, W. Yang, J. Shu, S. V. Sinogeikin, Y. Meng, D. Brewe, J. Z. Jiang, and H-k. Mao, Substitutional alloy of Ce and Al, *Proc. Natl. Acad. Sci.* doi:10.1073/pnas.0813328106, 2009.
7. **W. L. Mao**, H-k. Mao, Y. Meng, P. J. Eng, M. Y. Hu, P. Chow, J. Shu, and R. J. Hemley, X-ray-induced dissociation of H₂O and formation of an O₂-H₂ alloy at high pressure, *Science* **314**, 636-638, 2006.
8. **W. L. Mao**, G. Shen, V. B. Prakapenka, Y. Meng, A. J. Campbell, D. L. Heinz, J. Shu, R. Hemley, and H-k. Mao, Ferromagnesian postperovskite silicates in the D'' layer of the Earth, *Proc. Nat. Acad. Sci.* **101**, 15867-15869, 2004.
9. **W. L. Mao**, H-k. Mao, P. J. Eng, T. P. Trainor, M. Newville, C-c. Kao, D. L. Heinz, J. Shu, Y. Meng, and R. Hemley, Bonding changes in compressed superhard graphite, *Science* **302**, 425-427, 2003.

Name: Shelly D. Kelly



Education/Training:

Institution and Location	Degree	Year	Field of Study
University of Washington	Ph.D	1999	Physics
University of Idaho	B.A.	1992	Physics

Research and Professional Experience:

<u>EXAFS Analysis</u>	Sole proprietor	March 2002-present
<u>UOP LLC, a Honeywell Company</u>	Consultant Physicist	March 2002-present
<u>Michigan State University</u>	Consultant Physicist	Dec 2008-present
<u>Argonne National Laboratory</u>	Postdoc	March 1999-April 2003
	Assistant Physicist	April 2003-March 2008
	Physicist	March 2008-August 2009

Professional Activities:

- Reviewer of General User Proposals on the Microprobe and Imaging Panel for the APS
- Reviewer of scientific manuscripts for Applied Physics Letters, Geochimica et Cosmochimica Acta, Environmental Science and Technology, American Mineralogist, Chemical Geology, Contaminant Hydrology, Journal of Synchrotron Radiation, Adsorption of Metals to Geomedia II, and Journal of Catalysis.
- Reviewer of proposals for Natural Environment Research Council Research (NERC), National Science Foundation (NSF), and Stanford Synchrotron Radiation Light Source (SSRL).
- EXAFS workshop instructor for the past 8 years at the National Synchrotron Light Source, 2002, 2003, and 2004 and at the Advanced Photon Source, 2005, 2006, and 2007, 2008, 2009.
- Organizer of "Future Directions in Synchrotron Environmental Science" at the Advance Photon Source Users Meeting, May 2004.
- Chair of Synchrotron-Based Analytical Techniques for Nuclear and Environmental Sciences session at the American Chemical Society 225th Meeting, New Orleans, LA, March 2003.
- Early Career Subcommittee member, Strategic Environmental Initiative, Argonne National Laboratory, 2002.
- Taught XAFS analysis and data collection at the National School on Neutron and X-ray Scattering, Advance Photon Source, August 12-25, 2001.

Selected Publications:

1. Kelly, S. D. (2010). Uranium Chemistry in Soils and Sediments. *Synchrotron-based Techniques in Soil and Sediment*. Grafe, M. and Singh, B., Elsevier B.V. 34: 411-466.
2. Kelly, S. D., Wu, W. M., Yang, F., Criddle, C. S., Marsh, T. L., O'Loughlin, E. J., Ravel, B., Watson, D., Jardine, P. M. and Kemmer, K. M. (2010). "Uranium Transformation in Static Microcosms." *Environ. Sci. & Technol.* 44: 236-242.
3. Kelly, S. D., Yang, N., Mickelson, G. E., Greenlay, N., Karapetrova, E., Sinkler, W. and Bare, S. R. (2009). "Structural characterization of Ni-W hydrocracking catalysts using in situ EXAFS and HRTEM." *Journal of Catalysis* 263(1): 16-33.
4. Kelly, S. D., Hesterberg, D. and Ravel, B. (2008). Analysis of soils and minerals using X-ray absorption spectroscopy. *Methods of soil analysis, Part 5 -Mineralogical methods*. Ulery, A. L. and Drees, L. R. Madison, WI, USA, *Soil Science Society of America*: 367-463.
5. Kelly, S. D., Kemner, K. M., Carley, J., Criddle, C., Jardine, P. M., Marsh, T. L., Phillips, D., Watson, D. and Wu, W. M. (2008). "Speciation of uranium in sediments before and after in situ biostimulation." *Environmental Science & Technology* 42(5): 1558-1564.
6. Kelly, S. D., Kemner, K. M. and Brooks, S. C. (2007). "X-ray Absorption Spectroscopy Identifies Calcium-Uranyl-Carbonate Complexes at Environmental Concentrations." *Geochimica Et Cosmochimica Acta* 71(4): 821-834.
7. Kelly, S. D., Rasbury, E. T., Chattopadhyay, S., Kropf, A. J. and Kemner, K. M. (2006). "Evidence of a Stable Uranyl Site in Ancient Organic-Rich Calcite." *Environmental Science & Technology* 40(7): 2262-2268.

Name: Satish C. B. Myneni

Education/Training:

Institution and Location	Degree	Year	Field of Study
The Ohio State University	Ph.D.	1995	Environmental Geochemistry
Indian Inst. of Tech., Kharagpur	M. Tech.	1991	Applied Geology
Indian Inst. of Tech., Bombay	M. Sc.	1989	Applied Geology

Research and Professional Experience:

<u>Princeton University</u>		
Associate Professor		2005-present
Assistant Professor		1999-2005
<u>Lawrence Berkeley National Laboratory</u>		
Geological Scientist		1998-1999
Postdoctoral Scientist		1995-1998

Professional Activities last 5 years:

Reviewer for grant proposals of USDA, DOE, NSF
Member of the American Chemical Society, Geochemical Society
Review Panels
Proposal Review Panel (2005-present) & Proposal Oversight Panel (2007-present), National Synchrotron Light Source
DOE (3 times in the last 5 years)

Significant Awards and Honors

1985-87 Merit scholarship, Indian Institute of Technology, Bombay
1992 Outstanding teaching associate award, The Ohio State University
2001 Best research paper on interfacial processes in the environment, BES, DOE.

Five Selected Publications

1. *Tropical dendrochemistry: A novel approach to estimate age and growth from ringless trees.* Poussart P.M., Myneni S.C.B., Lanzirrotti A. *Geophys. Res. Let.* **33** (17) (2006) L17711.
2. *Effect of soil fulvic acid on nickel (II) sorption and bonding at the aqueous-boehmite (γ -AlOOH) interface.* Strathmann T.J., Myneni S.C.B. *Environ. Sci. Technol.* **39**: (2005) 4027-4034.
3. *Organic aerosol growth mechanisms and their climate forcing implications.* Maria S., Russell L.M., Gilles M.K., Myneni S.C.B. *Science* 306: (2004) 1921-1924.
4. *Formation of stable chlorinated hydrocarbons in weathering plant material.* Myneni S.C.B. *Science* 295: (2002) 1039-1041
5. *Imaging of Humic Substance Macromolecular Structures in Water and Soils.* Myneni S.C.B., Brown J., Martinez G.A., and Meyer-Ilse. W. *Science* 286: (1999) 1335-1337.

Name: Bhoopesh Mishra

Education/Training:

Institution and Location	Degree	Year	Field of Study
University of Notre Dame (IN, USA)	Ph.D	2006	Physics
Indian Institute of Technology (Bombay, India)	M.Sc	2000	Physics
Science College, Patna University (Patna, India)	B.Sc	1998	Physics

Research and Professional Experience:

<u>Argonne National Laboratory</u> Postdoctoral Research Associate, Biosciences Division	Aug. 2009 -present
<u>Princeton University</u> Postdoctoral Research Associate, Department of Geosciences	Aug. 2006-Aug. 2009
<u>University of Notre Dame</u> Research Assistant/Fellow, Department of Physics	Aug. 2000- Aug. 2006

Professional Activities:

- Reviewer for *Environmental Science and Technology*, *Water Research*, *Journal of Environmental Engineering*, *Geochimica et Cosmochimica Acta*, *Biometals*, and *Chemical Geology*.
- Associate Editor of *Geochemical News* since January 2009
- Guest Editor for the special issue of the journal *BioMetals* on “Siderophores: From Biogeochemistry to Medical perspectives”
- Reviewer of *National Science Foundation (NSF)*, *Geobiology and Low-temperature Geochemistry* program

Recent Publications:

1. **Bhoopesh Mishra**, Jeremy Fein, Nathan Yee, Terry J. Beveridge, Satish C.B. Myneni “Hg-Cysteine Complexation on Bacterial Cell Walls” (Submitted to *Nature Geoscience*)
2. **Bhoopesh Mishra**, Maxim I. Boyanov, Bruce A. Bunker,, Shelly D. Kelly, Kenneth M. Kemner, and Jeremy B. Fein “High- and low-affinity binding sites for Cd on the bacterial cell walls of *Bacillus subtilis* and *Shewanella oneidensis*” *Geochimica et Cosmochimica Acta*, 2010, (In press, [doi:10.1016/j.gca.2010.02.019](https://doi.org/10.1016/j.gca.2010.02.019))
3. **Bhoopesh Mishra**, Elizabeth A. Haack, Patricia A. Maurice, Bruce A. Bunker, "Effects of Microbial siderophore DFO-B on Pb Adsorption to Kaolinite" *Chemical Geology*, 2010, (In press, [doi:10.1016/j.chemgeo.2010.05.009](https://doi.org/10.1016/j.chemgeo.2010.05.009))
4. **Bhoopesh Mishra**, Maxim I. Boyanov, Bruce A. Bunker,, Shelly D. Kelly, Kenneth M. Kemner, Robert Nerenberg, Brenda L. Read-Daily, and Jeremy B. Fein “An X-ray Absorption Spectroscopy Study of Cd Binding Onto Bacterial Consortia” *Geochimica et Cosmochimica Acta*, **73**(15), 4311-4325 (2009)
5. Thomas Wichard, **Bhoopesh Mishra**, Satish C.B. Myneni, Jean-Phillipe Bellenger, Anne M.L. Kraepiel, “Storage and bioavailability of Mo in soils increased by organic matter complexation” *Nature Geoscience*, **2**, 625-629 (2009)
6. **Bhoopesh Mishra**, Elizabeth A. Haack, Patricia A. Maurice, Bruce A. Bunker, “Effects of Microbial Siderophore DFO-B on Pb and Cd Speciation in Aqueous Solution” *Environmental Science and Technology*, **43**(1), 94-100 (2009)
7. (*Invited Review*) Patricia Maurice, Elizabeth Haack, **Bhoopesh Mishra**, “Siderophores Sorption to Clays” *BioMetals*, **22**(4), 649-658 (2009)
8. John Komlos, **Bhoopesh Mishra**, Antonio Lanzirrotti, Satish C.B. Myneni and Peter R. Jaff , “Real Time Speciation of Uranium during Active Bioremediation and U(IV) Reoxidation” *Journal of Environmental Engineering*, **134**(2), 78-86 (2008)
9. Debdutta Lahiri, Bruce Bunker, **Bhoopesh Mishra**, Zhenyuan Zhang, Dan Meisel, C.M. Doudna, M.F. Bertini, Frank D. Blum, A.T. Tokuhira, Soma Chattopadhyay, Tomohiro Shibata, Jeff Terry, “Bimetallic Pt-Ag and Pd-Ag nanoparticles”, *Journal of Applied Physics*, **97**, (9), 943041-943047 (2005)